treated with TAT-PEG liposomes (Cy3-labeled pDNA: 3 μg/mL) and FITC-CTB (10 μg/mL) for 1 h at 37 °C. After incubation, the cells were washed, and BLs (120 μg/mL) were added. US exposure was then applied (frequency, 2028 kHz; duty, 50%; burst rate, 2.0 Hz; intensity, 1.0 W/cm^2; time, 10 s). Subsequently, the cells were incubated for 10, 60, or 180 min and then fixed with 4% paraformaldehyde for 1 h at 4 °C. CLSM was then performed (FV1000D; Olympus Corporation, Tokyo, Japan).

RESULTS

Characterization of Prepared TAT-PEG Liposomes. We evaluated the average size and zeta potential of prepared TAT-PEG liposomes, which were about 130 nm with a slight positive charge (Table 1).

Table 1. Characteristics of Prepared Liposomes[a]

prepared liposomes	PEG liposomes	TAT-PEG liposomes
particle size (nm)	132.1 ± 6.5	122.5 ± 10.5
ζ potential (mV)	3.17 ± 1.7	7.91 ± 1.6

[a]Data are the means and SD of three different determinations.

Cellular Association of TAT-PEG Liposomes. We first confirmed the effect of TAT peptide coating on the cellular association of liposomes and examined the association of TAT-PEG liposomes with HeLa cells. The cells were incubated with DiI-labeled liposomes for 1 h at 37 °C, and fluorescence intensity was determined by flow cytometry. The cellular internalization of TAT-PEG liposomes was observed by confocal laser scanning microscopy (CLSM). The cells treated with TAT-PEG liposomes showed increased fluorescence intensities compared with nonlabeled PEG liposomes (Figure 1A). In cells treated with TAT-PEG liposomes, the fluorescence of liposomes was observed in the cytoplasm, whereas it was weak in the cytoplasm of cells treated with nonlabeled PEG liposomes (Figure 1B). Furthermore, we investigated the cellular uptake pathway of TAT-PEG liposomes. Inhibitors that block clathrin-mediated endocytosis, raft-dependent endocytosis, and macropinocytosis were used to determine the cellular uptake pathway of TAT-PEG liposomes. Clathrin-mediated endocytosis was inhibited by chlorpromazine, which prevents the assembly of coated pits at the plasma membrane.[15] Raft-dependent endocytosis was inhibited by genistein, which is a thyrosine

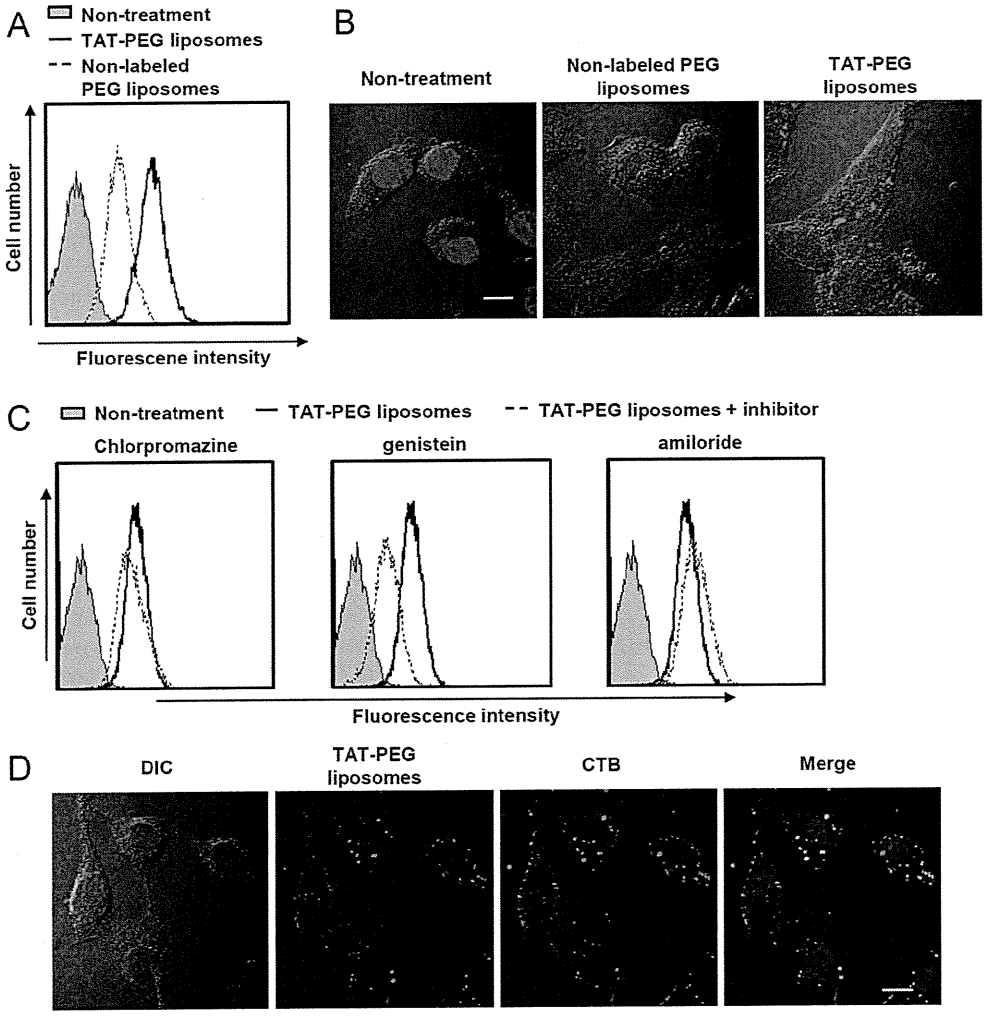

Figure 1. Cellular association of TAT-PEG liposomes. (A, B) HeLa cells were treated with DiI-labeled nonlabeled or TAT-PEG liposomes for 1 h at 37 °C. (A) The fluorescence intensity was measured by flow cytometry. (B) Cells were observed by CLSM. The scale bar represents 10 μm. (C) Cells were incubated with chlorpromazine (10 μg/mL), genistein (400 μM), or amiloride (1 mM) for 30 min and then treated with DiI-labeled TAT-PEG liposomes in the presence of an endocytic inhibitor for a further 1 h at 37 °C. Fluorescence intensities were measured by flow cytometry. (D) Cells were treated with DiI-labeled nonlabeled or TAT-PEG liposomes in the presence of FITC-CTB (10 μg/mL) for 1 h at 37 °C. Cells were observed by CLSM. The scale bar represents 10 μm.

kinase inhibitor.[16] We also used amiloride, a specific inhibitor of the Na^+/H^+ exchange required for macropinocytosis.[17] Flow cytometry analysis showed that the fluorescence intensity of TAT-PEG liposomes in the cells was decreased when cells were treated with genistein. In contrast, the fluorescence intensity of TAT-PEG liposomes in the cells was not changed when cells were treated with chlorpromazine or amiloride (Figure 1C). Furthermore, to elucidate the intracellular localization of TAT-PEG liposomes, the cells were treated with DiI-labeled TAT-PEG liposomes and FITC-cholera toxin B subunit (FITC-CTB), a marker of raft-dependent endocytosis,[18] and then observed by CLSM. As a result, the fluorescence of TAT-PEG liposomes was colocalized with the fluorescence of CTB in cells treated with TAT-PEG liposomes and CTB for 1 h (Figure 1D).

Gene Transfection by TAT-PEG Liposomes. Although TAT-PEG liposomes could be internalized efficiently into cells via raft-dependent endocytosis, it was necessary to achieve high gene expression so that genes in the endosome were delivered into the cytoplasm. To assess the ability of endosomal escape in TAT-PEG liposomes, the cells were treated with TAT-PEG liposomes in the presence of chloroquine, which is recognized as an endosomolytic agent.[19] Luciferase activity was 100-fold higher than that following treatment with TAT-PEG liposomes in the absence of chloroquine (Figure 2). It was suggested that

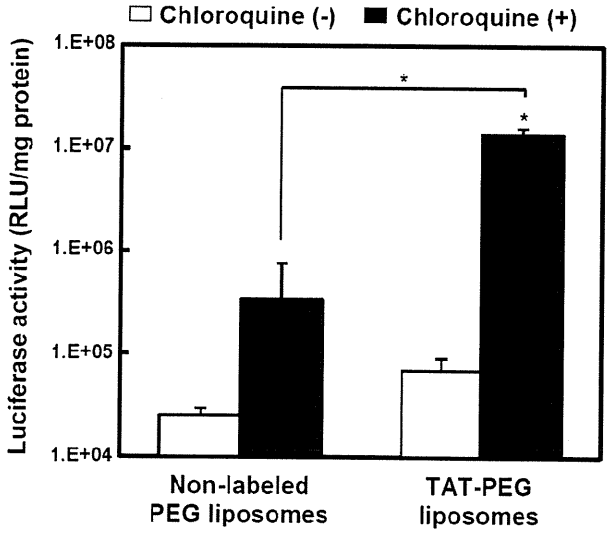

Figure 2. Gene transfection by TAT-PEG liposomes. Cells were preincubated with chloroquine (100 μM) for 30 min before transfection and then treated with nonlabeled or TAT-PEG liposomes in the presence of chloroquine for a further 4 h at 37 °C. After replacement with fresh medium, the cells were cultured for 20 h, and then luciferase activity was determined. Scale bars represent 10 μm. Data are the means ± SD ($n = 4$). *$p < 0.05$ compared with treatment in the absence of chloroquine.

the TAT-PEG liposomes prepared in this study could be efficiently internalized into cells but might not release genes into the cytoplasm from endosomes.

Effects of BLs and US Exposure on the Transfection Efficiency of TAT-PEG Liposomes. To investigate the effect of BLs and US exposure on TAT-mediated liposomal gene transfection, HeLa cells were treated with TAT-PEG liposomes for 4 h at 37 °C in a serum-free medium, and then the cells were treated with BLs and US exposure. After treatment with TAT-PEG liposomes, luciferase activity was enhanced up to 30-fold by BLs and US exposure compared with TAT-PEG liposomes alone. Furthermore, the combination of TAT-PEG liposomes with BLs and US exposure had about 10-fold higher luciferase activity than nonlabeled PEG liposomes with BLs and US exposure (Figure 3A). We also examined the transfection efficiency by treating TAT-PEG liposomes with US in the absence of BLs. As a result, the transfection efficiency was barely enhanced by treatment with TAT-PEG liposomes with US compared with TAT-PEG liposomes alone (Figure 3B). The cytotoxicity of the combination of TAT-PEG liposomes with or without BLs and US exposure was determined using a WST-8 assay. The cell viability was more than 80% even after each transfection (Figure 3C,D). It was suggested that BLs and US exposure could enhance the transfection efficiency of TAT-PEG liposomes without significant cytotoxicity.

Mechanism of Gene Transfection by TAT-PEG Liposomes with BLs and US Exposure. We examined the effects of BLs and US exposure on the cellular uptake of TAT-PEG liposomes. Flow cytometry analysis was performed to measure the fluorescence intensity of Cy3-labeled pDNA in cells transfected by TAT-PEG liposomes with or without BLs and US exposure. As a result, the cellular uptake of pDNA showed almost no difference in the presence of TAT-PEG liposomes with or without BLs and US exposure (Figure 4A). To evaluate the involvement of the direct induction of TAT-PEG liposomes into cells, the cells were transfected with TAT-PEG liposomes with or without BLs and US exposure at 37 or 4 °C. Twenty-three hours after transfection, luciferase activity was measured. When the cells were transfected by TAT-PEG liposomes with BLs and US exposure at 37 °C, the luciferase activity increased compared with that of cells treated with TAT-PEG liposomes alone. In contrast, luciferase activity did not change in cells treated with TAT-PEG liposomes with BLs and US exposure at 4 °C compared with TAT-PEG liposomes alone (Figure 4B). We also confirmed the effect of temperature on the cellular uptake of TAT-PEG liposomes. The cells were treated with DiI-labeled TAT-PEG liposomes for 1 h at 37 °C or at 4 °C, and then fluorescence intensity was measured by flow cytometry. In cells treated at 4 °C, fluorescence intensity decreased compared with cells treated at 37 °C (data not shown). To evaluate the intracellular distribution of pDNA, HeLa cells were treated with TAT-PEG liposomes containing Cy3-labeled pDNA in the presence of FITC-CTB for 1 h, and then the cells were treated with BLs and US exposure. After US exposure, the cells were incubated for 10, 60, or 180 min and observed by CLSM. In cells treated with TAT-PEG liposomes alone, the fluorescence of pDNA colocalized with the fluorescence of CTB. In contrast, when cells were treated with BLs and US exposure, the fluorescence of CTB was dispersed widely in cells that were incubated for 10 min after US exposure (Figure 4C). We also confirmed the intracellular distribution of pDNA and CTB in living cells. As a result, the distribution of pDNA and CTB in living cells was similar to that of fixed cells (data not shown). Furthermore, we examined the intracellular distribution of pDNA and CTB treated by TAT-PEG liposomes with US in the absence of BLs. The intracellular distribution of pDNA and CTB showed almost no difference between the treatment of TAT-PEG liposomes alone and TAT-PEG liposomes with US exposure without BLs (data not shown).

It was suggested that BLs and US exposure could affect the intracellular trafficking of pDNA and enhance the transfection efficacy of TAT-PEG liposomes.

dx.doi.org/10.1021/mp200353m | Mol. Pharmaceutics 2011, 8, 2416–2423

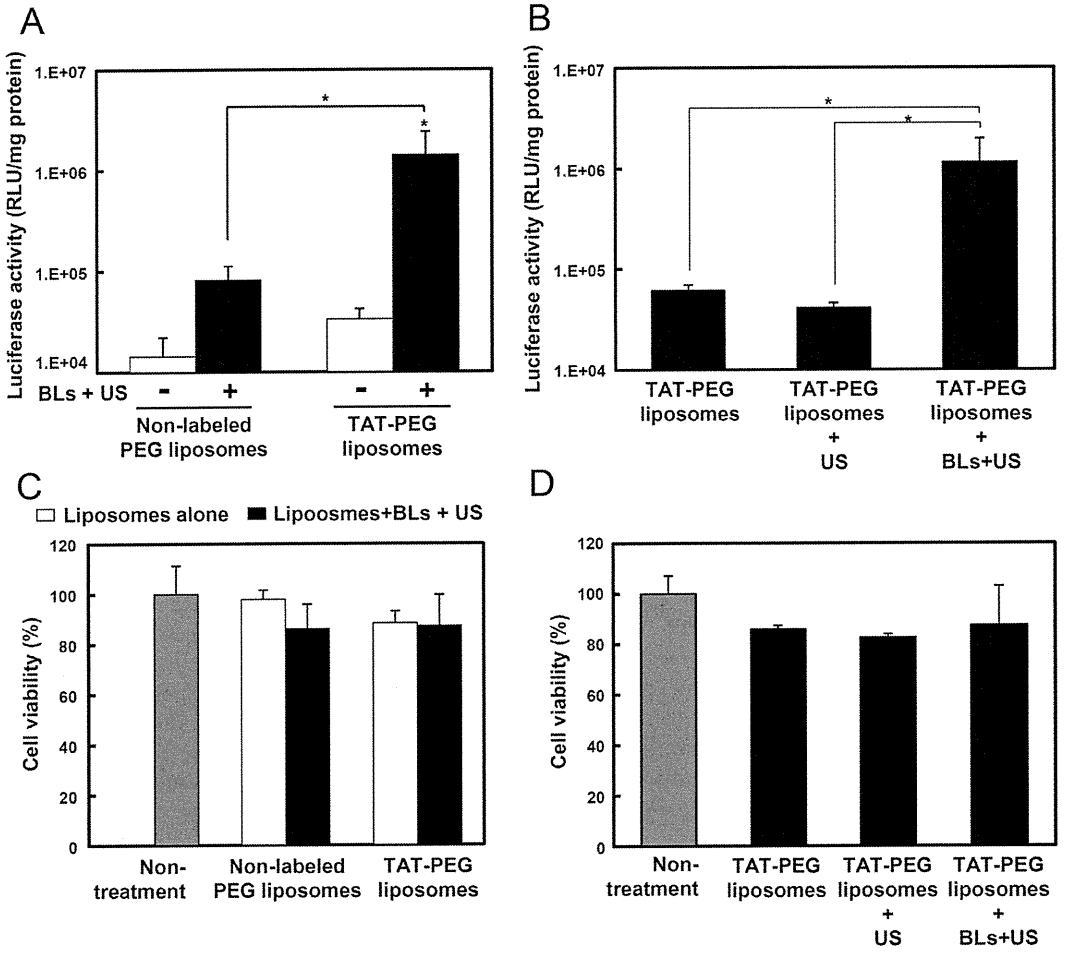

Figure 3. Effect of BLs and US exposure on TAT-mediated liposomal gene transfection. HeLa cells were treated with nonlabeled or TAT-PEG liposomes for 4 h. The cells were then washed and treated with or without BLs (120 μg/mL) and US exposure. They were incubated for 20 h; then (A, B) luciferase activity was determined, and (C, D) cell viability was measured using a WST-8 assay. Data are the means ± SD (n = 4). *p < 0.05 compared with TAT-PEG liposomes alone.

DISCUSSION

Recent studies have suggested that endosomal escape is important to achieve efficient gene delivery.[2,3] We have previously reported that BLs and US exposure could improve the transfection efficiency of laminin-derived AG73-PEG liposomes containing pDNA by promoting endosomal escape.[9] In this report, we demonstrated that BLs and US exposure could enhance not only the transfection efficiency of AG73-PEG liposomes but also that of TAT-PEG liposomes.

For efficient gene delivery, various moieties were used to develop carriers which enhance cellular internalization or selectivity. CPPs, such as TAT, R8, or penetratin, were used to achieve efficient gene internalization.[12,20,21] On the other hand, for selective gene delivery, folate, transferrin, RGD, or anisamide was used as a ligand.[22−25] These moieties were associated with a specific receptor and internalized via several endocytoses. TAT peptide was associated with heparan sulfate proteoglycan, which has been controversial.[26] In addition, some studies have developed TAT peptide-modified carriers, which were equipped with components enhancing endosomal escape;[14] therefore, we focused on TAT peptide and evaluated whether BLs and US exposure can enhance the transfection efficiency of TAT peptide-modified carriers to demonstrate the utility of BLs and US exposure in general. The present results showed that BLs and US exposure could enhance the gene transfection efficiency of TAT-PEG liposomes (Figure 3A). Furthermore, although we have previously reported that AG73-PEG liposomes were partially internalized via clathrin-mediated endocytosis,[9] the TAT-PEG liposomes prepared in this study were mostly internalized via a raft-dependent endocytic pathway (Figure 1C). These results suggested that BLs and US exposure could enhance the transfection efficiency of vectors, which were internalized via various receptor and endocytic pathways; however, further studies are needed to evaluate the effect of BLs and US exposure on the transfection efficiency of vectors, which were internalized via various endocytic pathways, such as macropinocytosis.

For successful gene therapy, nonviral vectors could be needed to overcome rate-limiting steps, such as cellular internalization, endosomal escape, and nuclear transfer.[2,3] Endosomal escape is considered to be one of the most important steps. Although PEG modification was considered a useful component to increase the stability of vectors in vivo, it also inhibited endosomal escape, leading to decreased gene expression.[27,28] Our results also showed that TAT-PEG liposomes could not escape from endosomes to the cytosol efficiently (Figures 1D, 2). We previously reported that BLs and US exposure could enhance the endosomal escape of AG73-PEG liposomes.[9] We therefore further confirmed the effect of BLs and US exposure on endosomal escape of TAT-PEG liposomes. We and other

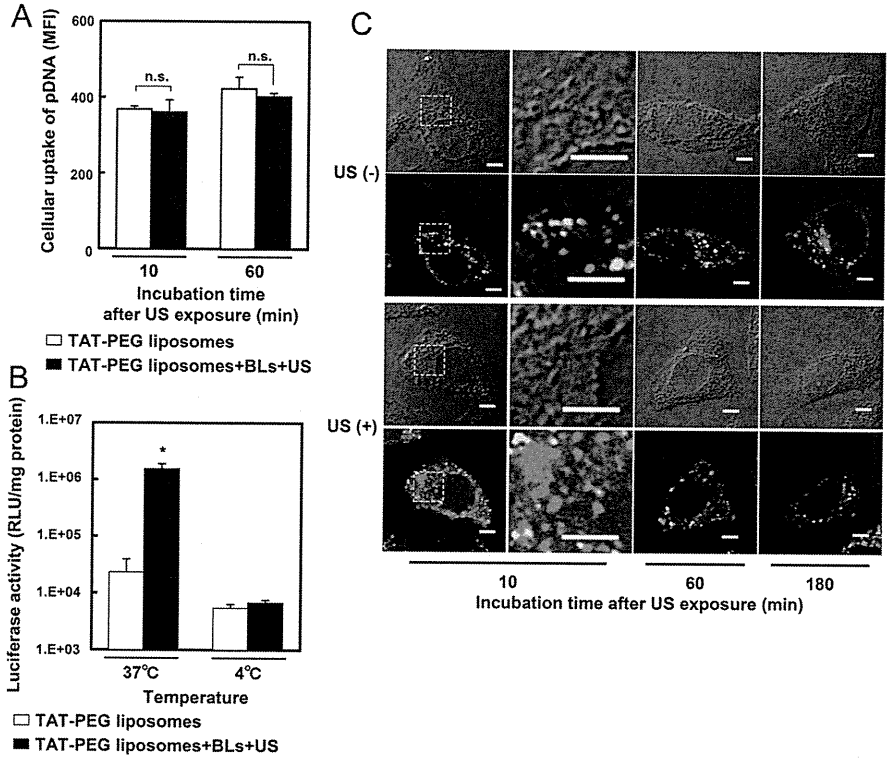

Figure 4. Mechanism of accelerated TAT-mediated liposomal gene transfection by BLs and US exposure. (A) HeLa cells were incubated with TAT-PEG liposomes encapsulating Cy3-labeled pDNA for 4 h at 37 °C. After incubation, the cells were washed, and BLs were added. Then the cells were exposed to US and incubated for 10 or 60 min. The cells were then collected and washed with heparin-containing PBS three times. The fluorescence intensity was measured by flow cytometry. Data are shown as the means ± SD (n = 3). (B) Cells were preincubated for 30 min at either 37 or 4 °C before transfection and then treated with TAT-PEG liposomes for a further 1 h at 37 or 4 °C. After incubation, the cells were washed, and BLs were added. The cells were then exposed to US and cultured for 23 h. Luciferase activity was determined. Data are the means ± SD (n = 4). *p < 0.05 compared with TAT-PEG liposomes alone. (C) Cells were treated with TAT-PEG liposomes encapsulating Cy3-labeled pDNA and FITC-CTB (10 μg/mL) for 1 h at 37 °C. After incubation, the cells were washed, and BLs were added. The cells were then exposed to US, incubated for 10, 60, 180 min, and then fixed with 4% paraformaldehyde for 1 h at 4 °C and observed by CLSM. The areas surrounded by dotted line are shown as enlarged images. Scale bars represent 5 μm.

groups have reported that the combination of BLs or microbubbles with US exposure could increase cell membrane permeability and deliver genes into the cytosol directly;[29−33] however, our results indicated that enhanced transfection efficiency did not rely on the increase of the direct cellular uptake of TAT-PEG liposomes, which is associated with the cell membrane (Figure 4A). In addition, CLSM analysis showed that BLs and US exposure could affect intracellular trafficking of TAT-PEG liposomes. Although endocytic vesicles labeled with FITC-CTB were observed as punctuate structures, when BLs and US exposure was applied, it was observed that FITC-CTB diffused into the cytosol (Figure 4B). These results suggested that BLs and US exposure could accelerate endosomal escape of TAT-PEG liposomes. We also examined whether sonazoid (Daiichi-Sankyo Pharmaceuticals, Tokyo, Japan) and US exposure could enhance the transfection efficiency of TAT-PEG liposomes. Sonazoid consists of perfluorobutane gas microbubbles stabilized by a monolayer membrane of hydrogenated egg phosphatidyl serine.[34] As a result, the transfection efficiency of TAT-PEG liposomes was enhanced by sonazaoid and US exposure (data not shown). This result suggested that microbubbles and US exposure could enhance the gene transfection efficiency of gene delivery carriers.

We also prepared folate-PEG liposomes containing pDNA and examined whether BLs and US exposure could enhance the transfection efficiency of folate-PEG liposomes. Folate, a high-affinity ligand for folate receptor, has been widely used as a ligand for selective gene delivery, and folate-modified carriers required various components enhancing endosomal escape to achieve high gene transfection efficiency.[35] We confirmed that folate-PEG liposomes had relatively low transfection efficiency because of the lower ability of endosomal escape, but when BLs and US exposure was used with folate-PEG liposomes, the transfection efficiency of folate-PEG lisposomes was enhanced (data not shown). These findings also suggested that BLs and US exposure could enhance the endosomal escape of gene delivery vectors, leading to increased gene expression.

We have reported that the transfection efficiency of AG73-PEG liposomes using BLs and US exposure was enhanced 60-fold,[9] whereas that of TAT-PEG liposomes was up-regulated 12-fold (Figure 3A). These results suggested that BLs and US exposure could easily influence the intracellular trafficking of AG73-PEG liposomes compared to TAT-PEG liposomes. The different efficacy of endosomal escape between AG73-PEG liposomes and TAT-PEG liposomes might be dependent on the difference of the receptor, endocytic pathway of carrier, and the type of cells. The responsibility of BLs and US exposure to individual cells might also affect the efficiency of endosomal escape, leading to different transfection efficiencies; therefore, it is important to clarify the mechanism of the different efficacy of endosomal escape of these carriers. However, we expect that this method of promoting endosomal escape using BLs and US

dx.doi.org/10.1021/mp200353m | Mol. Pharmaceutics 2011, 8, 2416–2423

exposure may also be applied to existing carriers for drug, peptide, or protein delivery, which have low intracellular delivery efficacy due to poor endosomal escape.

In further studies, we will attempt to demonstrate the detailed mechanism of enhanced endosomal escape of carriers by treatment with BLs and US exposure. It has been demonstrated that microbubbles and US exposure induce several biological effects, such as influx of calcium ions or generation of reactive oxygen species.[36−39] It has been also reported that endosomal acidification is adjusted by calcium ions;[40] therefore, we will assess whether the influx of calcium ions induced by BLs and US exposure affects endosomal acidification and function, leading to the destabilization of endosomes and enhancement of endosomal escape. On the other hand, we may also need to elucidate more clearly the effect of BLs and US exposure on transcription and other organelles. Although it is possible that BLs and US exposure may induce several biological effects involved in gene expression, BLs and US exposure could affect the intracellular distribution of pDNA and CTB (Figure 4); therefore, our results suggested that BLs and US exposure could certainly improve at least the endosomal escape of TAT-PEG liposomes.

In conclusion, as schematically shown in Figure 5, TAT-PEG liposomes were internalized into cells via HSPG and raft-dependent endocytosis. On the other hand, AG73-PEG liposomes and folate-PEG liposomes were internalized via syndecan-2 and folate receptor, respectively. When BLs and US exposure were applied, endosomal escape was enhanced, leading to increased transfection efficiency of these carriers. These results suggested that BLs and US exposure could enhance transfection efficiency by promoting endosomal escape, which was independent of the receptors and endocytic pathway of carriers. Thus, BLs and US exposure can be useful tools to achieve efficient gene transfection by improving endosomal escape using various carriers.

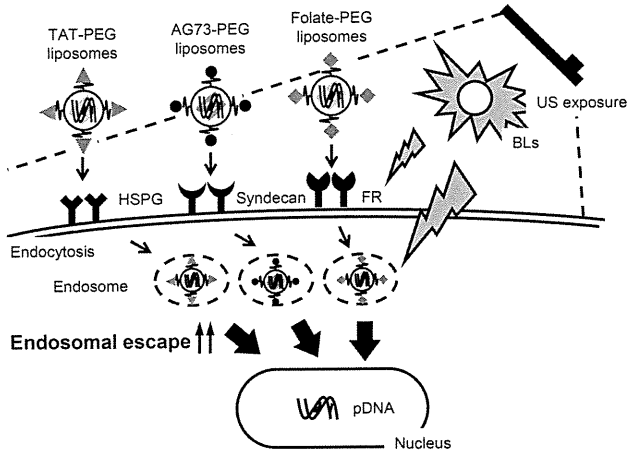

Figure 5. Diagram of enhanced gene delivery by BLs and US exposure. Several moiety-modified gene delivery carriers were internalized into cells via receptors and the endocytic pathway. When BLs and US exposure were applied, endosomal escape was enhanced, leading to increased transfection efficiency, which was independent of the receptor and endocytic pathway of carriers. HSPG, heparan sulfate proteoglycan; FR, folate receptor; US, ultrasound; BLs, Bubble liposomes; PEG, poly(ethylene glycol).

AUTHOR INFORMATION

Corresponding Author

*Mailing address: Tokyo University of Pharmacy and Life Sciences, School of Pharmacy, 1432-1 Horinouchi, Hachioji, Tokyo 192-0392, Japan. Tel. and fax: +81-42-676-3183. E-mail address: negishi@toyaku.ac.jp (Y.N.).

ACKNOWLEDGMENTS

We are grateful to Dr. Katsuro Tachibana (Department of Anatomy, School of Medicine, Fukuoka University) for technical advice regarding the induction of cavitation with US and to Mr. Yasuhiko Hayakawa, Mr. Takahiro Yamauchi, and Mr. Kosho Suzuki (NEPA GENE CO., LTD.) for technical advice regarding exposure to US. This study was supported by an Industrial Technology Research Grant (04A05010) from the New Energy and Industrial Technology Development Organization (NEDO) of Japan, Grant-in-Aid for Exploratory Research (18650146) and Grant-in-Aid for Scientific Research (B) (20300179) from the Japan Society for the Promotion of Science, and by a grant for private universities provided by the Promotion and Mutual Aid Corporation for Private Schools of Japan.

ABBREVIATIONS

BLs, Bubble liposomes; CTB, cholera toxin B subunit; DOPE, 1,2-dioleoyl-sn-glycero-3-phosphoethanolamine; DOPG, 1,2-dioleoyl-*sn*-glycero-3-phospho-*rac*-1-glycerol; DSPE, 1,2-distearoyl-*sn*-glycero-3-phosphatidyl-ethanolamine; FBS, fetal bovine serum; Fmoc, fluorenylmethoxycarbonyl; Mal, maleimide; pDNA, plasmid DNA; PEG, poly(ethylene glycol); US, ultrasound

REFERENCES

(1) Zhang, S.; Xu, Y.; Wang, B.; Qiao, W.; Liu, D.; Li, Z. Cationic compounds used in lipoplexes and polyplexes for gene delivery. *J. Controlled Release* **2004**, *100*, 165−180.

(2) Hama, S.; Akita, H.; Ito, R.; Mizuguchi, H.; Hayakawa, T.; Harashima, H. Quantitative comparison of intracellular trafficking and nuclear transcription between adenoviral and lipoplex systems. *Mol. Ther.* **2006**, *13*, 786−794.

(3) Varga, C. M.; Tedford, N. C.; Thomas, M.; Klibanov, A. M.; Griffith, L. G.; Auffenburger, D. A. Quantitative comparison of polyethylenimine formulations and adenoviral vectors in terms of intracellular gene delivery processes. *Gene Ther.* **2005**, *12*, 1023−1032.

(4) Hatakeyama, H.; Ito, E.; Akita, H.; Oishi, M.; Nagasaki, Y.; Futaki, S.; Harashima, H. A pH-sensitive fusogenic peptide facilitates endosomal escape and greatly enhances the gene silencing of siRNA-containing nanoparticles in vitro and in vivo. *J. Controlled Release* **2009**, *139*, 127−132.

(5) Subbarao, N. K.; Parente, R. A.; Szoka, F. C.; Nadasdi, L.; Pongracz, K. pH-dependent bilayer destabilization by an amphipathic peptide. *Biochemistry* **1987**, *26*, 2964−2972.

(6) Lee, S. H.; Choi, S. H.; Kim, S. H.; Park, T. G. Thermally sensitive cationic polymer nanocapsules for specific cytosolic delivery and efficient gene silencing of siRNA: swelling induced physical disruption of endosome by cold shock. *J. Controlled Release* **2008**, *125*, 25−32.

(7) Høgset, A.; Prasmickaite, L.; Selbo, P. K.; Hellum, M.; Engesaeter, B. Ø.; Bonsted, A.; Berg, K. Photochemical internalisation in drug and gene delivery. *Adv. Drug Delivery Rev.* **2004**, *56*, 95−115.

(8) Negishi, Y.; Omata, D.; Iijima, H.; Hamano, N.; Endo-Takahashi, Y.; Nomizu, M.; Aramaki, Y. Preparation and characterization of laminin-derived peptide AG73-coated liposomes as a selective gene delivery tool. *Biol. Pharm. Bull.* **2010**, *33*, 1766−1769.

(9) Negishi, Y.; Omata, D.; Iijima, H.; Takabayashi, Y.; Suzuki, K.; Endo, Y.; Suzuki, R.; Maruyama, K.; Nomizu, M.; Aramaki, Y. Enhanced laminin-derived peptide AG73-mediated liposomal gene transfer by Bubble liposomes and ultrasound. *Mol. Pharmaceutics* **2010**, *7*, 217–226.

(10) Katayama, S.; Hirose, H.; Takayama, K.; Nakase, I.; Futaki, S. Acylation of octaarginine: Implication to the use of intracellular delivery vectors. *J. Controlled Release* **2011**, *149*, 29–35.

(11) Dey, D.; Inayathullah, M.; Lee, A. S.; Lemieux, M. C.; Zhang, X.; Wu, Y.; Nag, D.; De Almeida, P. E.; Han, L.; Rajadas, J.; Wu, J. C. Efficient gene delivery of primary human cells using peptide linked polyethylenimine polymer hybrid. *Biomaterials* **2011**, *32*, 4647–4658.

(12) Yamano, S.; Dai, J.; Yuvienco, C.; Khapli, S.; Moursi, A. M.; Montclare, J. K. Modified Tat peptide with cationic lipids enhances gene transfection efficiency via temperature-dependent and caveolae-mediated endocytosis. *J. Controlled Release* **2011**, *152*, 278–285.

(13) Zeng, X.; Sun, Y. X.; Qu, W.; Zhang, X. Z.; Zhuo, R. X. Biotinylated transferrin/avidin/biotinylated disulfide containing PEI bioconjugates mediated p53 gene delivery system for tumor targeted transfection. *Biomaterials* **2010**, *31*, 4771–4780.

(14) Suk, J. S.; Suh, J.; Choy, K.; Lai, S. K.; Fu, J.; Hanes, J. Gene delivery to differentiated neurotypic cells with RGD and HIV Tat peptide functionalized polymeric nanoparticles. *Biomaterials* **2006**, *27*, 5143–5150.

(15) Wang, L. H.; Rothberg, K. G.; Anderson, R. G. Mis-assembly of clathrin lattices on endosomes reveals a regulatory switch for coated pit formation. *J. Cell. Biol.* **1993**, *123*, 1107–1117.

(16) Pelkmans, L.; Püntener, D.; Helenius, A. Local actin polymerization and dynamin recruitment in SV40-induced internalization of caveolae. *Science* **2002**, *296*, 535–539.

(17) Wadia, J. S.; Stan, R. V.; Dowdy, S. F. Transducible TAT-HA fusogenic peptide enhances escape of TAT-fusion proteins after lipid raft macropinocytosis. *Nat. Med.* **2004**, *10*, 310–315.

(18) Janes, P. W.; Ley, S. C.; Magee, A. I. Aggregation of lipid rafts accompanies signaling via the T cell antigen receptor. *J. Cell. Biol.* **1999**, *147*, 447–461.

(19) Sonawane, N. D.; Szoka, F. C.; Verkman, A. S. Chloride accumulation and swelling in endosomes enhances DNA transfer by polyamine-DNA polyplexes. *J. Biol. Chem.* **2003**, *278*, 44826–44831.

(20) Kibria, G.; Hatakeyama, H.; Ohga, N.; Hida, K.; Harashima, H. Dual-ligand modification of PEGylated liposomes shows better cell selectivity and efficient gene delivery. *J. Controlled Release* **2011**, *153*, 141–148.

(21) Mäe, M.; El Andaloussi, S.; Lundin, P.; Oskolkov, N.; Johansson, H. J.; Guterstam, P.; Langel, U. A stearylated CPP for delivery of splice correcting oligonucleotides using a non-covalent co-incubation strategy. *J. Controlled Release* **2009**, *134*, 221–227.

(22) Morris, V. B.; Sharma, C. P. Folate mediated l-arginine modified oligo (alkylaminosiloxane) graft poly(ethyleneimine) for tumor targeted gene delivery. *Biomaterials* **2011**, *32*, 3030–3041.

(23) Koppu, S.; Oh, Y. J.; Edrada-Ebel, R.; Blatchford, D. R.; Tetley, L.; Tate, R. J.; Dufes, C. Tumor regression after systemic administration of a novel tumor-targeted gene delivery system carrying a therapeutic plasmid DNA. *J. Controlled Release* **2010**, *143*, 215–221.

(24) Ng, Q. K.; Sutton, M. K.; Soonsawad, P.; Xing, L.; Cheng, H.; Segura, T. Engineering clustered ligand binding into nonviral vectors: $\alpha v\beta 3$ targeting as an example. *Mol. Ther.* **2009**, *17*, 828–836.

(25) Li, S. D.; Chono, S.; Huang, L. Efficient oncogene silencing and metastasis inhibition via systemic delivery of siRNA. *Mol. Ther.* **2008**, *16*, 942–946.

(26) Imamura, J.; Suzuki, Y.; Gonda, K.; Roy, C. N.; Gatanaga, H.; Ohuchi, N.; Higuchi, H. Single Particle Tracking Confirms That Multivalent Tat Protein Transduction Domain-induced Heparan Sulfate Proteoglycan Cross-linkage Activates Rac1 for Internalization. *J. Biol. Chem.* **2011**, *286*, 10581–10592.

(27) Hatakeyama, H.; Akita, H.; Kogure, K.; Oishi, M.; Nagasaki, Y.; Kihira, Y.; Ueno, M.; Kobayashi, H.; Kikuchi, H.; Harashima, H. Development of a novel systemic gene delivery system for cancer therapy with a tumor-specific cleavable PEG-lipid. *Gene Ther.* **2007**, *14*, 68–77.

(28) Walker, G. F.; Fella, C.; Pelisek, J.; Fahrmeir, J.; Boeckle, S.; Ogris, M.; Wagner, E. Toward synthetic viruses: endosomal pH-triggered deshielding of targeted polyplexes greatly enhances gene transfer in vitro and in vivo. *Mol. Ther.* **2005**, *11*, 418–425.

(29) Negishi, Y.; Matsuo, K.; Endo-Takahashi, Y.; Suzuki, K.; Matsuki, Y.; Takagi, N.; Suzuki, R.; Maruyama, K.; Aramaki, Y. Delivery of an angiogenic gene into ischemic muscle by novel Bubble liposomes followed by ultrasound exposure. *Pharm. Res.* **2011**, *28*, 712–719.

(30) Suzuki, R.; Namai, E.; Oda, Y.; Nishiie, N.; Otake, S.; Koshima, R.; Hirata, K.; Taira, Y.; Utoguchi, N.; Negishi, Y.; Nakagawa, S.; Maruyama, K. Cancer gene therapy by IL-12 gene delivery using liposomal bubbles and tumoral ultrasound exposure. *J. Controlled Release* **2010**, *142*, 245–250.

(31) Lentacker, I.; Wang, N.; Vandenbroucke, R. E.; Demeester, J.; De Smedt, S. C.; Sanders, N. N. Ultrasound Exposure of Lipoplex Loaded Microbubbles Facilitates Direct Cytoplasmic Entry of the Lipoplexes. *Mol. Pharmaceutics* **2009**, *6*, 457–467.

(32) Negishi, Y.; Endo, Y.; Fukuyama, T.; Suzuki, R.; Takizawa, T.; Omata, D.; Maruyama, K.; Aramaki, Y. Delivery of siRNA into the cytoplasm by liposomal bubbles and ultrasound. *J. Controlled Release* **2008**, *132*, 124–130.

(33) Taniyama, Y.; Tachibana, K.; Hiraoka, K.; Aoki, M.; Yamamoto, S.; Matsumoto, K.; Nakamura, T.; Ogihara, T.; Kaneda, T.; Morishita, R. Development of safe and efficient novel nonviral gene transfer using ultrasound: enhancement of transfection efficiency of naked plasmid DNA in skeletal muscle. *Gene Ther.* **2002**, *9*, 372–380.

(34) Otani, K.; Yamahara, K.; Ohnishi, S.; Obata, H.; Kitamura, S.; Nagaya, N. Nonviral delivery of siRNA into mesenchymal stem cells by a combination of ultrasound and microbubbles. *J. Controlled Release* **2009**, *133*, 146–153.

(35) Shi, G.; Guo, W.; Stephenson, S. M.; Lee, R. J. Efficient intracellular drug and gene delivery using folate receptor-targeted pH-sensitive liposomes composed of cationic/anionic lipid combinations. *J. Controlled Release* **2002**, *80*, 309–319.

(36) Juffermans, L. J.; Dijkmans, P. A.; Musters, R. J.; Visser, C. A.; Kamp, O. Transient permeabilization of cell membranes by ultrasound-exposed microbubbles is related to formation of hydrogen peroxide. *Am. J. Physiol. Heart Circ. Physiol.* **2006**, *291*, H1595–H1601.

(37) Juffermans, L. J.; Kamp, O.; Dijkmans, P. A.; Visser, C. A.; Musters, R. J. Low-intensity ultrasound-exposed microbubbles provoke local hyperpolarization of the cell membrane via activation of BK(Ca) channels. *Ultrasound Med. Biol.* **2008**, *34*, 502–508.

(38) Zhou, Y.; Shi, J.; Cui, J.; Deng, C. X. Effects of extracellular calcium on cell membrane resealing in sonoporation. *J. Controlled Release* **2008**, *126*, 34–43.

(39) Kumon, R. E.; Aehle, M.; Sabens, D.; Parikh, P.; Han, Y. W.; Kourennyi, D.; Deng, C. X. Spatiotemporal effects of sonoporation measured by real-time calcium imaging. *Ultrasound Med. Biol.* **2009**, *35*, 494–506.

(40) Lelouvier, B.; Puertollano, R. Mucolipin-3 regulates luminal calcium, acidification, and membrane fusion in the endosomal pathway. *J. Biol. Chem.* **2011**, *286*, 9826–9832.

Pharm Res (2011) 28:712–719
DOI 10.1007/s11095-010-0286-4

RESEARCH PAPER

Delivery of an Angiogenic Gene into Ischemic Muscle by Novel Bubble Liposomes Followed by Ultrasound Exposure

Yoichi Negishi • Keiko Matsuo • Yoko Endo-Takahashi • Kentaro Suzuki • Yuuki Matsuki • Norio Takagi • Ryo Suzuki • Kazuo Maruyama • Yukihiko Aramaki

Received: 31 July 2010 / Accepted: 15 September 2010 / Published online: 8 October 2010

ABSTRACT

Purpose To develop a safe and efficient gene delivery system into skeletal muscle using the combination of Bubble liposomes (BL) and ultrasound (US) exposure, and to assess the feasibility and the effectiveness of BL for angiogenic gene delivery in clinical use.

Methods A solution of luciferase-expressing plasmid DNA (pDNA) and BL was injected into the tibialis (TA) muscle, and US was immediately applied to the injection site. The transfection efficiency was estimated by a luciferase assay. The ischemic hindlimb was also treated with BL and US-mediated intramuscular gene transfer of bFGF-expressing plasmid DNA. Capillary vessels were assessed using immunostaining. The blood flow was determined using a laser Doppler blood flow meter.

Results Highly efficient gene transfer could be achieved in the muscle transfected with BLs, and US mediated the gene transfer. Capillary vessels were enhanced in the treatment groups with this gene transfer method. The blood flow in the treated groups with this gene transfer method quickly recovered compared to other treatment groups (non-treated, bFGF alone, or bFGF+US).

Conclusion The gene transfer system into skeletal muscle using the combination of BL and US exposure could be an effective means for angiogenic gene therapy in limb ischemia.

KEY WORDS angiogenesis · bubble liposomes · gene delivery · ultrasound

INTRODUCTION

Skeletal muscle is a candidate target tissue for the gene therapy of both muscle (*e.g.*, Duschenne Muscular dystrophy) and non-muscle disorders (*e.g.*, cancer, ischemia, or arthritis). Its usefulness is due mainly to its stability and longevity after a gene transfer, which make it a good target tissue for gene therapy via the production of therapeutic proteins such as cytoskeletal proteins, trophic factors, or hormones. To achieve successful gene therapy in a clinical setting, it is critical that gene delivery systems be safe, easy to apply, and provide therapeutic transgene expression. Several previous studies using viral vectors reported the successful transfer of therapeutic genes into the target cells, but because of the considerable immunogenicity related to the use of viruses, non-viral gene transfer still needs to be developed (1). Recently, among physical non-viral gene transfer methods, it has been shown that therapeutic ultrasound enables genes to permeate cell membranes. The mechanism of gene transfer is believed to be involved in an acoustic cavitation (2–6). However, to achieve efficient gene transfer, a high

Yoichi Negishi and Keiko Matsuo have contributed equally to this work.

Y. Negishi (✉) • K. Matsuo • Y. Endo-Takahashi • K. Suzuki •
Y. Matsuki • Y. Aramaki
Department of Drug and Gene Delivery Systems
School of Pharmacy, Tokyo University of Pharmacy and Life Sciences
1432-1 Horinouchi, Hachioji
Tokyo 192-0392, Japan
e-mail: negishi@toyaku.ac.jp

N. Takagi
Department of Molecular and Cellular Pharmacology
School of Pharmacy, Tokyo University of Pharmacy and Life Sciences
1432-1 Horinouchi, Hachioji
Tokyo 192-0392, Japan

R. Suzuki • K. Maruyama
Department of Pharmaceutics, Teikyo University
1091-1 Suwarashi, Midori-ku
Sagamihara, Kanagawa 252-5195, Japan

intensity of US is required, which leads to tissue damage (7,8). In contrast, low-intensity US in combination with microbubbles has recently acquired much attention as a safe method of gene delivery (9–13). However, microbubbles have problems with size, stability, and targeting function. Liposomes have been known as drug, antigen, and gene delivery carriers (14–18). To solve the above-mentioned issues of microbubbles, we previously developed the polyethyleneglycol (PEG)-modified liposomes entrapping echo-contrast, "bubble liposomes" (BL), which can function as a novel gene delivery tool by applying them with US exposure (19–24).

In the present study, we developed a safe and efficient gene delivery system into skeletal muscle using the combination of BL and US exposure. We assessed the feasibility and the effectiveness of BL for gene therapy by trying to deliver a bFGF-expressing plasmid into skeletal muscle in a hindlimb ischemia model through the combination of BL and US exposure.

MATERIALS AND METHODS

Materials

Preparation of Bubble Liposomes

Bubble liposomes were prepared by the previously described methods (19,22). Briefly, PEG liposomes composed of 1, 2-dipalmitoyl-*sn*-glycero-3-phosphocholine (DPPC) (NOF Corporation, Tokyo, Japan) and 1,2-distearoyl-*sn*-glycero-3-phosphatidyl-ethanolamine-polyethyleneglycol (DSPE-PEG_{2000}-OMe) (NOF corporation, Tokyo, Japan) in a molar ratio of 94:6 were prepared by a reverse phase evaporation method. In brief, all reagents were dissolved in 1:1 (v/v) chloroform/diisopropyl ether. Phosphate-buffered saline was added to the lipid solution, and the mixture was sonicated and then evaporated at 47°C. The organic solvent was completely removed, and the size of the liposomes was adjusted to less than 200 nm using extruding equipment and a sizing filter (pore size: 200 nm) (Nuclepore Track-Etch Membrane, Whatman plc, UK). The lipid concentration was measured using a Phospholipid C test Wako (Wako Pure Chemical Industries, Ltd., Osaka, Japan). BL were prepared from liposomes and perfluoropropane gas (Takachio Chemical Ind. Co. Ltd., Tokyo, Japan). First, 2-mL sterilized vials containing 0.8 mL of liposome suspension (lipid concentration: 1 mg/mL) were filled with perfluoropropane gas, capped, and then pressurized with a further 3 mL of perfluoropropane gas. The vial was placed in a bath-type sonicator (42 kHz, 100 W) (BRANSONIC 2510j-DTH, Branson Ultrasonics Co., Danbury, CT, USA) for 5 min to form BL.

Plasmid DNA (pDNA)

The plasmid pcDNA3-Luc, derived from pGL3-basic (Promega, Madison, WI), is an expression vector encoding the firefly luciferase gene under the control of a cytomegalovirus promoter. The plasmid pEGFP-N3 (Clontech Laboratories, Inc., Mountain View, CA) is an expression vector encoding the enhanced green fluorescein protein under the control of a cytomegalovirus promoter. The plasmid pBLAST-hbFGF (InvivoGen Inc.) is an expression vector encoding human bFGF under the control of an EF-1α promoter.

In Vivo Gene Delivery into the Skeletal Muscle of Mice with BL and US

ICR mice (5 weeks old, male) were anesthetized with pentobarbital throughout each procedure. A 40 μl suspension of pDNA (10 μg) and BL (30 μg) was injected into the tibialis (TA) muscle of the ICR mice, and US exposure (frequency: 1 MHz; duty: 50%; intensity: 2 W/cm^2; time: 60 s) was immediately applied at the injection site. A Sonitron 2000 (NEPA GENE, CO, LTD) was used as an ultrasound generator. Several days after the injection, the mice were euthanized and sacrificed, and the tibialis muscle in the US-exposed area was collected and homogenized. The cell lysate and tissue homogenates were prepared with a lysis buffer (0.1 M Tris-HCl (pH 7.8), 0.1% Triton X-100, and 2 mM EDTA). Luciferase activity was measured using a luciferase assay system (Promega, Madison, WI) and a luminometer (LB96V, Belthold Japan Co. Ltd., Tokyo, Japan). The activity is indicated as relative light units (RLU) per mg of protein. For analyzing EGFP expression, the treated muscle was fixed with paraformaldehyde and dehydrated in a sucrose solution. The specimens were embedded in an OCT compound and immediately frozen at −80°C. Serial sections 8 μm thick were cut by cryostat and observed with a fluorescence microscope (Axiovert 200 M, Carl Zeiss).

In Vivo Luciferase Imaging

The mice were anaesthetized and *i.p.* injected with D-luciferin (150 mg/kg) (Xenogen, Corporation, CA). After 10 min, luciferase expression was observed with an *in vivo* luciferase imaging system (IVIS) (Xenogen Corporation).

Tissue-Damage Testing Using Evans-Blue Dye (EBD)

Tissue-damage testing using EBD was performed as previously reported (25). Briefly, EBD was dissolved in PBS (10 mg/ml) and sterilized by using 0.2 μm membrane filters. Mice treated with pDNA, BL, and US exposure were administered with the dissolved EBD (0.5 mg dye per

10 g body weight) by tail vein injection. The mice were sacrificed 1 day after dye injection. The TA muscles were removed and photographed using a digital camera. The TA muscles were embedded in an OCT compound and immediately frozen at –80°C. Serial sections 10 μm thick were cut by cryostat and observed with a fluorescence microscope (Axiovert 200 M, Carl Zeiss).

Hindlimb Ischemia Model

The ischemic hindlimb model was created in five-week-old male ICR mice as previously reported (26). Briefly, animals were anesthetized, and a skin incision was made in the left hindlimb. After ligation of the proximal end of the femoral artery at the level of the inguinal ligament, the distal portion and all the side branches were dissected free and excised. The right hindlimb was kept intact to control the original blood flow. Immediately after ischemia was induced, a mixture of 40 μl of a pDNA (10 μg of pBLAST-hbFGF or pBLAST as an control vector) and BL (30 μg) suspension was injected into the adductor muscle of the ischemia mice, and US exposure (1 MHz, 2 w/cm^2, 50% duty cycle, 60 s) was immediately applied at the injection site. Measurements of the ischemic (left)/normal (right) limb blood flow ratio were performed for a set time using a laser Doppler blood flow meter (OMEGAFLO, FLO-C1).

bFGF ELISA

bFGF secretion was determined as previously reported (27). Briefly, 5- to 6-week-old male ICR mice were anesthetized by intraperitoneal injection of pentobarbital. The leg was shaved and depilated to expose the tibialis anterior muscle. Ten micrograms of DNA in a 40 μL bubble liposome or PBS solution were injected into the tibialis anterior muscle. After DNA injection, US exposure was applied. The tibialis anterior muscle was collected 2 days after the DNA injection. The muscle was washed three times in 3 mL of PBS to remove debris and blood. The washed muscle was placed in a 24-well plate coating growth factor reduced Matrigel (BD Biosciences) and incubated at 37°C. The muscle was grown in 1.5 mL of M199 medium containing 2% fetal bovine serum, 100 U/mL penicillin, and 100 mg/mL streptomycin. The levels of secreted cytokines in the conditioned media of the explants cultures were measured using human bFGF ELISA (R&D Systems), according to the manufacturer's instructions.

Immunohistochemistry

The ischemic thigh muscles were perfused on day 14 with PBS and 4% paraformaldehyde and embedded in paraffin. Muscle sections (4 μm) were stained with anti-CD31 antibody (BD pharmingen) overnight at 4°C. We then incubated the sections with Alexa Fluor 488 rabbit anti-rat IgG (Molecular Probes).

In Vivo Studies

Animal use and relevant experimental procedures were approved by the Tokyo University of Pharmacy and Life Science Committee and Teikyo University on the Care and Use of Laboratory Animals. All experimental protocols for animal studies were in accordance with the Principle of Laboratory Animal Care in Teikyo University.

Statistical Analyses

All data are shown as the mean±SD (n=4 or 6). Data were considered significant when $P<0.05$. The t-test was used to calculate statistical significance.

RESULTS

In Vivo Gene Delivery into the Skeletal Muscle of Mice with BL and US Exposure

It has been reported that microbubbles improve tissue permeability by cavitation upon US exposure. We first tried to deliver the naked pDNA (pCMV-Luc) into tibialis muscle using BL and US. A solution of pDNA and BL was injected into TA muscle, and US was immediately applied to the injection site, as shown in Fig. 1. As a result, the relative luciferase activity was high in the group treated using the pDNA plasmid with BL and US exposure. In contrast, there was low activity in the groups treated with pDNA alone, pDNA+BL, or pDNA+US. The luciferase activity in the group receiving a combination of BL with US exposure was 200- or 20-fold higher than that of the group treated with pDNA alone or pDNA + US, respectively (Fig. 1a). We next investigated whether their gene expression was derived from muscle cells. In a similar fashion, the EGFP expression plasmid (pEGFP-N3) was delivered into TA muscle, and 5 days after the gene delivery, the EGFP expression was sectioned and examined by fluorescent microscopy. As shown in Fig. 1b, the intramuscular gene delivery of the EGFP expression plasmid by BL and US exposure was present in a wide area of the positive muscle fibers of EGFP. In contrast, in the muscle specimens of the other treated groups (pDNA alone, pDNA+BL, or pDNA+US), very little expression was shown (Fig. 1b). We also observed the luciferase gene expression area in the whole body using an *in vivo* luciferase imaging system at 5 days after the transfection into the muscle treated with pDNA, BL, and US exposure.

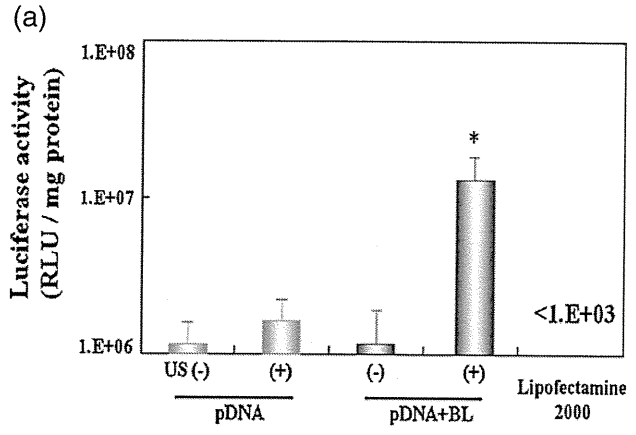

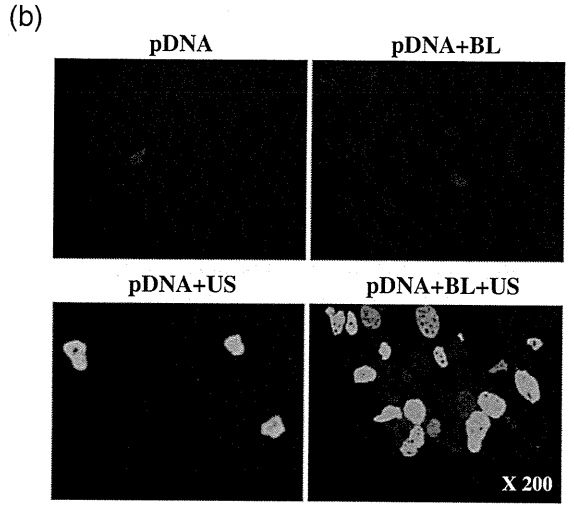

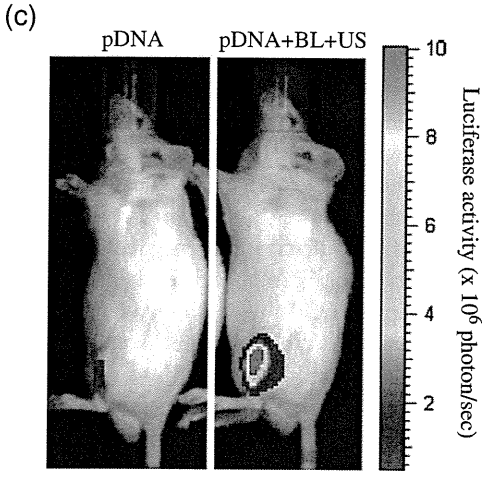

◀ **Fig. 1** Reporter gene expression after BL and US-mediated gene transfer compared with Lipofectamine 2000. (a) Luciferase expression after BL and US-mediated gene transfer compared with Lipofectamine 2000. Mice were treated with BL and US-mediated intramuscular luciferase gene transfer or Lipofectamine 2000. Five days after transfection, luciferase expression was determined. In another experiment, a pDNA (pCMV-Luc (10 μg))-Lipofectamine 2000 (25 μg) complex was suspended in PBS and injected into the left femoral artery. *$P < 0.01$ compared to the group of pDNA alone, pDNA + US, pDNA + BL, or Lipofectamine 2000 with BL. pDNA (pCMV-Luciferase): 10 μg, BL: 30 μg. US exposure (Frequency: 1 MHz, Duty: 50%, Intensity: 2 W/cm^2, Time: 60 s). (b) EGFP expression after BL and US-mediated gene transfer. Mice were treated with BL and US-mediated intramuscular EGFP gene transfer. Five days after transfection, EGFP expression was analyzed by fluorescent microscopy. Each of the gene transfer conditions are indicated above the pictures. Magnification: x 200. (c) photon counts are indicated by the pseudo-color scales.

Although the level of gene expression gradually decreased 2 weeks after the transfection using BL and US exposure, the moderate gene expression persisted for 4 weeks after the transfection (data not shown). The gene expression was restricted to the area of US exposure (Fig. 1c). This suggested that the combination of BL and US exposure facilitated the efficient transfection of pDNA into the muscle due to the induction of cavitation. We also assessed the tissue damage by testing EBD uptake in the muscle transfected with the BL and US exposure; however, significant tissue damage was not observed at the US condition (frequency: 1 MHz; duty: 50%; intensity: 2 W/cm^2; time: 60 s), even in the presence of the cavitation by BL and US exposure (Fig. 2b, e). When a higher US intensisty (4 W/cm^2) was applied, significant tissue damage was detected (Fig. 2c, f).

In Vivo Effects of the bFGF Expression System

We next attempted to deliver bFGF plasmid into tibialis muscle using BL and US and determine the bFGF protein expression in explant culture medium. The amount of bFGF protein was high in the group treated with bFGF plasmid with BL and US exposure. In contrast, there was low expression in the group treated with bFGF plasmid alone, or bFGF plasmid+US (Fig. 3). We further investigated the capillary density in order to know the effects of BL and US-mediated gene delivery with bFGF plasmid injected intramuscularly into hindlimb ischemia model mice. In the treatment group with BL and US-mediated gene transfer, their capillary vessels with CD31 positive cells were significantly increased compared to the treatment group of the control plasmid (empty vector), the bFGF plasmid alone, or bFGF plasmid + US (Fig. 4a, b). Measurements of the ischemic (left)/non-ischemic (right) hindlimb blood flow ratio were further performed for a period of time using a laser Doppler blood flow meter. Consistent with this induction of angiogenesis, the blood flow in the group treated with the bFGF plasmid with BL and US exposure was significantly increased compared with the group treated with the control plasmid (empty vector), the bFGF plasmid alone, bFGF plasmid + US (Fig. 5). Although we also examined the blood flow ratio after treatment with US exposure alone or BL with US exposure

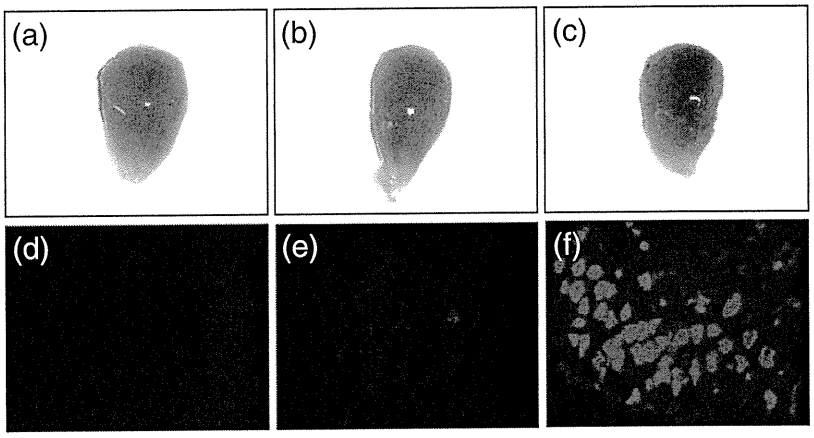

Fig. 2 Tissue-damage testing using EBD. pDNA alone without BL and US exposure (a, d). pDNA with BL and US exposure condition at a frequency of 1 MHz with an intensity of 2 W/cm^2 (b, e), or 4 W/cm^2 (c, f) for 60 s. The TA muscles were photographed using a digital camera (a, b, and c). Evans-blue fluorescence of 10 μm cryosections from the TA muscles was examined with fluorescence microscopy (d, e, and f). Magnification: ×100.

to the ischemic limb muscle, their blood flow ratio still remained in the 20 to 40% range. These results suggest that intramuscular injection of bFGF as an angiogenic gene with bubble liposomes followed by US exposure enabled us to improve an angiogenesis in the ischemic muscle.

DISCUSSION

The gene delivery of naked plasmid DNA is a feasible technique for non-viral gene therapy in a safe clinical use; however, a higher efficiency of site-specific delivery is required to achieve therapeutic effects in patients. In this view, we previously reported that BL is an efficient gene delivery tool (24,28,29). However, it is not enough to say that BL is a feasible and effective tool to carry out gene therapy to treat diseases. Here we demonstrate the development of a safe and efficient gene delivery system into skeletal muscle using the combination of BL and US exposure, and we assess the feasibility and the effectiveness of BL for angiogenic gene delivery. We therefore examined the potential ability of BL with US exposure to deliver a gene into skeletal muscle and its applicability for therapeutic angiogenesis in ischemic model. By using BL with US exposure, we first performed a transfer of luciferase-expressing plasmid DNA as a reporter plasmid into the TA muscle of mice. The remarkable gene expression could be enhanced efficiently only with the combination of both BL and US exposure when compared with other treatments (Fig. 1a). Exceeding our expectations, their gene expression was 200-fold higher than that of the plasmid DNA injection alone. When compared to Optison, one of the currently existing microbubbles (9–11), with US exposure, however, the gene transfer efficacy of BL was almost same as when using Optison (data not shown). Previously, our reports have demonstrated that the gene transfection efficiency *in vitro* could be affected with increasing the US intensity and the exposure time (20). The transfection efficiency increased with an increasing intensity of ultrasound and reached a plateau at 2 W/cm^2. No significant damage was observed under these conditions (Fig. 2b, e). When a higher intensity of US (4 W/cm^2) during the gene transfer with BL was applied to improve the transfection efficiency, the gene expression was conversely diminished (data not shown), and significant damage was also observed (Fig. 2c, f). This treatment caused significant tissue damage, probably due to the temperature elevation in the US exposure site. In this experiment, we therefore employed an US condition (frequency: 1 MHz; intensity: 2 W/cm^2; duty cycle: 50%; US exposure time: 1 min) that was in terms with a safety profile. As shown in Fig. 1b, the number of EGFP-positive muscle fibers could be apparently enhanced by the combination of BL and US

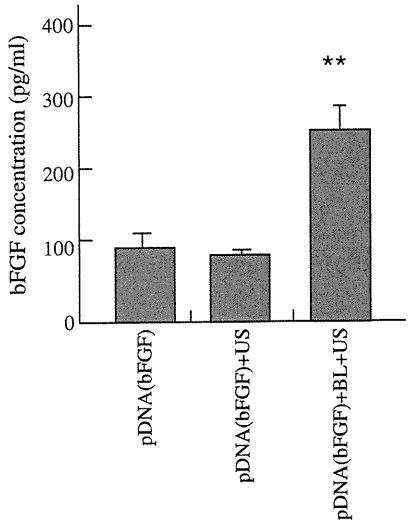

Fig. 3 bFGF protein expression after BL and US-mediated bFGF gene transfer. Mice were treated with BL and US-mediated intramuscular bFGF gene transfer. Two days after transfection, the muscle was collected and placed into Matrigel coating plates. After 3 days, the secreted bFGF protein expression was determined by ELISA. $^{**}P < 0.05$ *vs.* other treatment groups. pDNA (pBLAST-bFGF): 10 μg, BL: 30 μg, US exposure (Frequency: 1 MHz, Duty: 50%, Intensity: 2 W/cm^2, Time: 60 s).

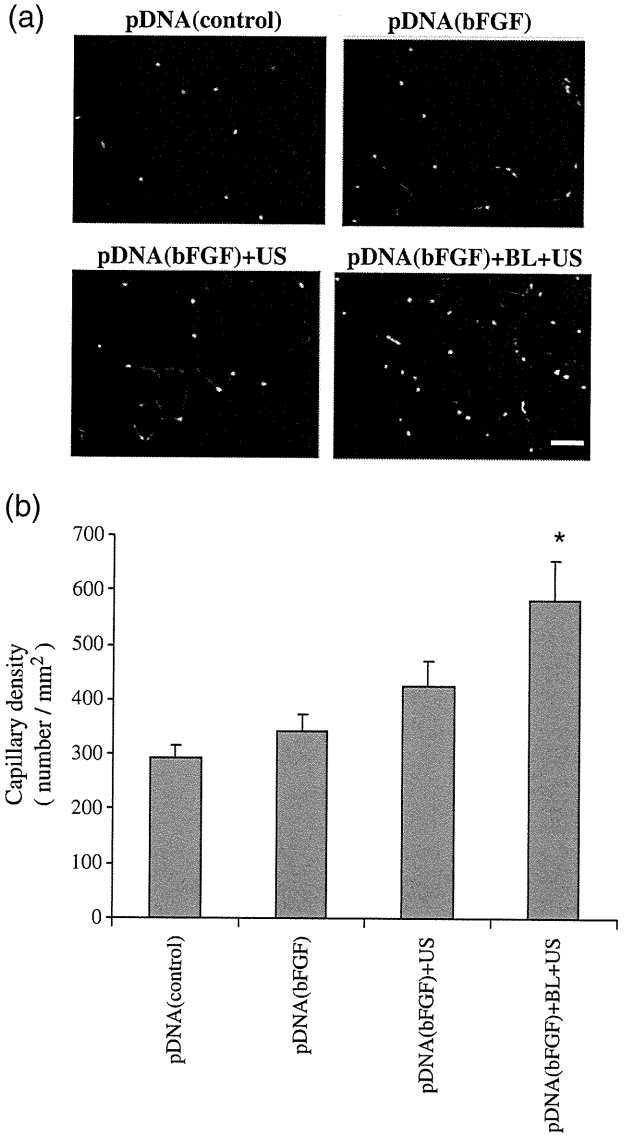

Fig. 4 Effect of BL and US-mediated bFGF gene transfer into hindlimb ischemia on capillary density. (a) CD31 staining of hindlimb muscle sections 14 days after BL and US-mediated bFGF gene transfer. The stained sections were analyzed by fluorescent microscopy. (b) CD31 positive vessels were measured. Green dots indicate CD31 positive vessels stained with an FITC-labeled anti-CD31 antibody. Scale bar represented 50 μm. *$P < 0.05$ vs. other treatment groups.

exposure; in contrast, without BL, only a few fibers could be observed in a treatment of US exposure without BL. Consequently, we found that a gene delivery method using BL and US exposure helped to both improve the transfection efficiency in the US focused site with a minimally invasive transfection procedure.

It is unclear whether BL with US exposure could improve transgene expression. Previously, we reported that BL could induce cavitation by a short duration (1–10 s) of US exposure and lead to efficient gene transfer into various types of cells (19,20). Therefore, the major biological effect of BL for gene delivery into the muscle may be through a cavitation induction, as was shown in previous reports (19). In contrast, in the case of Lipofectamine 2000, a commercial cationic lipid that is widely used in gene delivery, the transfection efficiency in the muscle was markedly lowered (Fig. 1a). This result is consistent with reports that serum proteins interact with and disturb cationic liposomes (29). It is expected that more time is required for this transfection, because cationic lipid/pDNA complexes (lipoplex) are entered into the cytoplasm by an endosomal pathway. Therefore, when the lipoplex with Lipofectamine 2000 was directly injected into the muscle, before it could enter into the cytoplasm by an endosomal pathway, it is possible that the degradation of pDNA or the aggregation of lipoplexes easily occurred. In contrast, once a solution of both BL and pDNA is administered into the muscle, US exposure is immediately applied at the injection site, leading to efficient gene expression, as shown in Fig. 1. In this way, unlike with lipoplexes, this simple method with BL and US exposure does not require a long time to achieve an efficient gene transfection. Our previous report has demonstrated that, by BL and US exposure, siRNA could directly enter into the cytoplasm without an endosomal pathway (22). In this report, because the level of gene expression corresponding

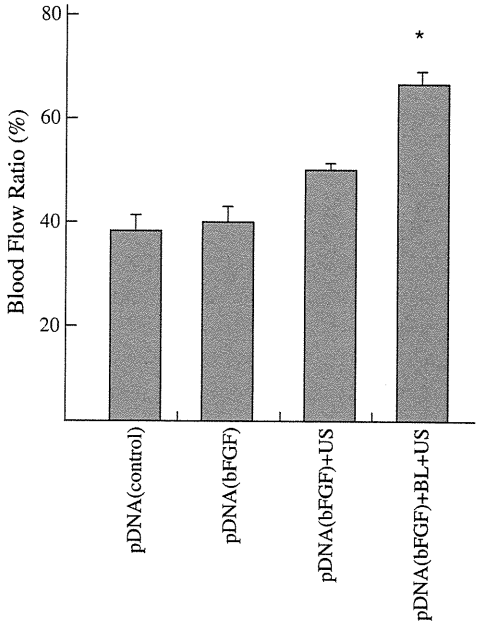

Fig. 5 Effect of BL and US-mediated bFGF gene transfer on the recovery of blood flow in ischemic limbs. After femoral artery ligation, mice were treated with BL and US-mediated intramuscular bFGF gene transfer. After the transfection, blood flow was measured at 14 days using a laser Doppler blood flow meter. *$P < 0.05$ vs. other treatment groups. Blood Flow Ratio (%): ischemic / normal blood flow ratio. pDNA (pBLAST-bFGF): 10 μg, BL: 30 μg, US exposure (Frequency: 1 MHz, Duty: 50%, Intensity: 2 W/cm^2, Time: 60 s).

to half of the expression in BL with a 1-minute US exposure could also be observed by BL with an only 10-second US exposure (data not shown), it may be thought that this transfection method by BL with US exposure enables immediate and direct pDNA delivery into the cytoplasm of muscle cells. The transfection efficiency might increase due to the appearance of transient holes in the cell membrane caused by the spreading of the BL, followed by their eruption with US exposure, which is consistent with previous reports using Optison (9).

Recently, a therapeutic strategy delivering angiogenic gene factors has been widely studied for clinical use in ischemic diseases (30). The delivery of naked plasmid DNA encoding an angiogenic gene into the ischemia has also been reported in clinical trials. However, the transfection efficiency is still insufficient for effective angiogenesis without side effects (30). Therefore, we assessed the feasibility and the effectiveness of BL for a gene therapy by trying to deliver a plasmid expressing bFGF, a key angiogenic factor, into the skeletal muscle of hindlimb ischemia model mice by the combination of BL and US exposure. As expected, with the gene delivery of the bFGF plasmid into an intramuscular injection with the combination of BL and US exposure, the capillary density and the blood flow ratio of the ischemic to non-ischemic hindlimb were markedly increased in the hindlimb transfected with the bFGF plasmid DNA through the combination of BL and a low intensity of US exposure compared to the plasmid DNA injection alone (Figs. 4 and 5). In addition, it has been reported that low-intensity US exposure can induce angiogenesis (31,32). However, no significant recovery in ischemic hindlimbs was observed with the combination of BL and US exposure without bFGF plasmid or with US exposure alone without the bFGF plasmid (data not shown). These results apparently indicate that therapeutic angiogenesis using naked plasmid DNA transfer that is enhanced by BL and US exposure could be a potential method in a clinical setting. We believe that there are several possibilities for BL usage in therapeutic angiogenesis with naked plasmid DNA in clinical use. The novel method using the combination of BL and US exposure may possibly reduce the amount of naked plasmid DNA, administration times, and the achievement of efficient gene transfer non-invasively without a viral vector, thereby enabling the decrease of the potential cost in clinical settings.

CONCLUSION

The present studies demonstrated a novel gene delivery method into skeletal muscle by the combination of BL and US exposure. Applied as gene therapy in a mouse model of ischemic limb muscle, intramuscular injection of bFGF as an angiogenic gene with BL followed by US exposure enabled improvement of an angiogenesis followed by apparent increased blood flow in the ischemic muscle. Because intramuscular injection of naked plasmid DNA alone may be inefficient and restrict its clinical use, this US-mediated BL technique may provide an effective non-invasive and non-viral method for angiogenic gene therapy for limb ischemia as well as for wound healing, ischemic heart disease, myocardial infarction, peripheral arterial diseases, and other various diseases.

ACKNOWLEDGEMENTS

We are grateful to Dr. Katsuro Tachibana (Department of Anatomy, School of Medicine, Fukuoka University) for technical advice regarding the induction of cavitation with US and to Mr. Yasuhiko Hayakawa, Mr. Takahiro Yamauchi, and Mr. Kosho Suzuki (NEPA GENE CO., LTD.) for technical advice regarding US exposure. This study was supported in part by the Industrial Technology Research Grant Program (04A05010) from New Energy, the Industrial Technology Development Organization (NEDO) of Japan, Grant-in-Aid for Scientific Research (B) (20300179) from the Japan Society of the Promotion of Science, and by a grant for private universities provided by the Promotion and Mutual Aid Corporation for Private Schools of Japan.

REFERENCES

1. Miller DG, Rutledge EA, Russell DW. Chromosomal effects of adeno-associated virus vector integration. Nat Genet. 2002;30:147–8.
2. Fechheimer M, Boylan JF, Parker S, Sisken JE, Patel GL, Zimmer SG. Transfection of mammalian cells with plasmid DNA by scrape loading and sonication loading. Proc Natl Acad Sci U S A. 1987;84:8463–7.
3. Miller MW, Miller DL, Brayman AA. A review of in vitro bioeffects of inertial ultrasonic cavitation from a mechanistic perspective. Ultrasound Med Biol. 1996;22:1131–54.
4. Joersbo M, Brunstedt J. Protein synthesis stimulated in sonicated sugar beet cells and protoplasts. Ultrasound Med Biol. 1990;16:719–24.
5. Greenleaf WG, Bolander ME, Sarkar G, Goldring MB, Greenleaf JF. Artificial cavitation nuclei significantly enhance acoustically induced cell transfection. Ultrasound Med Biol. 1998;24:587–95.
6. Schratzberger P, Krainin JG, Schratzberger G, Silver M, Ma H, Kearney M, *et al.* Transcutaneous ultrasound augments naked DNA transfection of skeletal muscle. Mol Ther. 2002;6:576–83.
7. Duvshani-Eshet M, Machluf M. Therapeutic ultrasound optimization for gene delivery: a key factor achieving nuclear DNA localization. J Control Release. 2005;108:513–28.
8. Kim HJ, Greenleaf JF, Kinnick RR, Bronk JT, Bolander ME. Ultrasound-mediated transfection of mammalian cells. Hum Gene Ther. 1996;7:1339–46.

9. Taniyama Y, Tachibana K, Hiraoka K, Aoki M, Yamamoto S, Matsumoto K, *et al.* Development of safe and efficient novel nonviral gene transfer using ultrasound: enhancement of transfection efficiency of naked plasmid DNA in skeletal muscle. Gene Ther. 2002;9:372–80.
10. Taniyama Y, Tachibana K, Hiraoka K, Namba T, Yamasaki K, Hashiya N, *et al.* Local delivery of plasmid DNA into rat carotid artery using ultrasound. Circulation. 2002;105:1233–9.
11. Li T, Tachibana K, Kuroki M, Kuroki M. Gene transfer with echo-enhanced contrast agents:comparison between Albunex, Optison, and Levovist in mice–initial results. Radiology. 2003;229:423–8.
12. Unger EC, Porter T, Culp W, Labell R, Matsunaga T, Zutshi R. Therapeutic applications of lipid-coated microbubbles. Adv Drug Deliv Rev. 2004;56:1291–314.
13. Sonoda S, Tachibana K, Uchino E, Okubo A, Yamamoto M, Sakoda K, *et al.* Gene transfer to corneal epithelium and keratocytes mediated by ultrasound with microbubbles. Invest Ophthalmol Vis Sci. 2006;47:558–64.
14. Blume G, Cevc G. Liposomes for the sustained drug release in vivo. Biochim Biophys Acta. 1990;1029:91–7.
15. Allen TM, Hansen C, Martin F, Redemann C, Yau-Young A. Liposomes containing synthetic lipid derivatives of poly(ethylene glycol) show prolonged circulation half-lives in vivo. Biochim Biophys Acta. 1991;1066:29–36.
16. Maruyama K, Yuda T, Okamoto A, Kojima S, Suginaka A, Iwatsuru M. Prolonged circulation time in vivo of large unilamellar liposomes composed of distearoyl phosphatidylcholine and cholesterol containing amphipathic poly(ethylene glycol). Biochim Biophys Acta. 1992;1128:44–9.
17. Maruyama K, Ishida O, Kasaoka S, Takizawa T, Utoguchi N, Shinohara A, *et al.* Intracellular targeting of sodium mercaptoundecahydrododecaborate (BSH) to solid tumors by transferrin-PEG liposomes, for boron neutron-capture therapy (BNCT). J Control Release. 2004;98:195–207.
18. Negishi Y, Omata D, Iijima H, Hamano N, Endo Y, Suzuki R, Maruyama K, Nomizu M, and Aramaki Y, Preparation and Characterization of Laminin-derived Peptide AG73-coated Liposomes as a Selective Gene Delivery Tool. *Biol Pham. Bull. in press*
19. Suzuki R, Takizawa T, Negishi Y, Hagisawa K, Tanaka K, Sawamura K, *et al.* Gene delivery by combination of novel liposomal bubbles with perfluoropropane and ultrasound. J Control Release. 2007;117:130–6.
20. Suzuki R, Takizawa T, Negishi Y, Utoguchi N, Sawamura K, Tanaka K, *et al.* Tumor specific ultrasound enhanced gene transfer in vivo with novel liposomal bubbles. J Control Release. 2008;125:137–44.
21. Suzuki R, Takizawa T, Negishi Y, Utoguchi N, Maruyama K. Effective gene delivery with novel liposomal bubbles and ultrasonic destruction technology. Int J Pharm. 2008;354:49–55.
22. Negishi Y, Endo Y, Fukuyama T, Suzuki R, Takizawa T, Omata D, *et al.* Delivery of siRNA into the cytoplasm by liposomal bubbles and ultrasound. J Control Release. 2008;132:124–30.
23. Negishi Y, Omata D, Iijima H, Takabayashi Y, Suzuki K, Endo Y, *et al.* Enhanced laminin-derived peptide AG73-mediated liposomal gene transfer by bubble liposomes and ultrasound. Mol Pharm. 2010;7:217–26.
24. Suzuki R, Namai E, Oda Y, Nishiie N, Otake S, Koshima R, *et al.* Cancer gene therapy by IL-12 gene delivery using liposomal bubbles and tumoral ultrasound exposure. J Control Release. 2010;142:245–50.
25. Liu F, Huang L. A syringe electrode device for simultaneous injection of DNA and electrotransfer. Mol Ther. 2002;5:323–8.
26. Couffinhal T, Silver M, Zheng LP, Kearney M, Witzenbichler B, Isner JM. Mouse model of angiogenesis. Am J Pathol. 1998;152:1667–79.
27. Jang HS, Kim HJ, Kim JM, Lee YS, Kim KL, Kim JA, *et al.* A novel *ex Vivo* angiogenesis assay based on electroporation-mediated delivery of naked plasmid DNA to skeletal muscle. Mol Ther. 2004;9:464–74.
28. Koch S, Pohl P, Cobet U, Rainov NG. Ultrasound enhancement of liposome-mediated cell transfection is caused by cavitation effects. Ultrasound Med Biol. 2000;26:897–903.
29. Yang JP, Huang L. Overcoming the inhibitory effect of serum on lipofection by increasing the charge ratio of cationic liposome to DNA. Gene Ther. 1997;4:950–60.
30. Shah PB, Losordo DW. Non-viral vectors for gene therapy: clinical trials in cardiovascular disease. Adv Genet. 2005;54:339–61.
31. Emoto M, Tachibana K, Iwasaki H, Kawarabayashi T. Antitumor effect of TNP-470, an angiogenesis inhibitor, combined with ultrasound irradiation for human uterine sarcoma xenografts evaluated using contrast color Doppler ultrasound. Cancer Sci. 2007;98:929–35.
32. Barzelai S, Sharabani-Yosef O, Holbova R, Castel D, Walden R, Engelberg S, *et al.* Low-intensity ultrasound induces angiogenesis in rat hind-limb ischemia. Ultrasound Med Biol. 2006;32:139–45.

International Journal of Pharmaceutics 422 (2012) 504–509

Contents lists available at SciVerse ScienceDirect

International Journal of Pharmaceutics

journal homepage: www.elsevier.com/locate/ijpharm

Pharmaceutical nanotechnology

Efficient siRNA delivery using novel siRNA-loaded Bubble liposomes and ultrasound

Yoko Endo-Takahashi[a,1], Yoichi Negishi[a,*,1], Yasuharu Kato[a], Ryo Suzuki[b], Kazuo Maruyama[b], Yukihiko Aramaki[a]

[a] Department of Drug Delivery and Biopharmaceutics, School of Pharmacy, Tokyo University of Pharmacy and Life Sciences, Hachioji, Tokyo, Japan
[b] Department of Biopharmaceutics, School of Pharmaceutical Sciences, Teikyo University, Sagamihara, Kanagawa, Japan

ARTICLE INFO

Article history:
Received 8 July 2011
Received in revised form 18 October 2011
Accepted 13 November 2011
Available online 22 November 2011

Keywords:
siRNA delivery
Ultrasound
Bubble liposomes

ABSTRACT

Recently, we developed novel polyethyleneglycol (PEG)-modified liposomes (Bubble liposomes; BLs) entrapping an ultrasound (US) imaging gas and reported that the combination of BLs and US was useful for the delivery of siRNA directly into the cytoplasm. However, the results were obtained using a mixture of BLs and naked siRNA. With systemic injections, it is important to control the biodistribution of both BLs and siRNA. In addition, the delivery of siRNA is affected by nuclease degradation after intravenous administration. In this study, we prepared novel siRNA-loaded BLs (si-BLs) using a cationic lipid, 1,2-dioleoyl-3-trimethylammonium-propane (DOTAP). We demonstrated that siRNA could be loaded onto BLs containing DOTAP and that siRNA-loaded BLs were stable in serum. A specific gene-silencing effect was also achieved by transfection with si-BLs. Thus, the combination of si-BLs with US exposure can be used for delivery of siRNA to a specific tissue via systemic injection.

1. Introduction

RNA interference (RNAi) has potential application in the development of new therapies for malignant, infectious, and autoimmune diseases. Indeed, synthetic siRNAs are capable of knocking down targets *in vivo* (Frank-Kamenetsky et al., 2008; Halder et al., 2006; Kim et al., 2008; McCaffrey et al., 2002; Morrissey et al., 2005; Niu et al., 2006; Sato et al., 2008; Song et al., 2003; Takeshita et al., 2005; Xia et al., 2007). However, effective and nontoxic delivery is the major challenge to its implementation in a clinical setting.

One novel approach to the administration of a drug or gene is ultrasound (US)-enhanced delivery, which exploits cavitation bubbles produced by the pressure oscillations of US. US pressures above a certain threshold can cause oscillating bubbles to collapse violently, a process known as inertial cavitation. Inertial cavitation is believed to temporarily improve the permeability of cell membranes, enabling the transport of extracellular molecules into viable cells (Delius and Adams, 1999; Duvshani-Eshet and Machluf, 2005; Greenleaf et al., 1998; Holmes et al., 1992; Schratzberger et al., 2002). Furthermore, in combination with microbubbles, contrast agents for medical US imaging improve siRNA transfection efficiency (Du et al., 2011; Kinoshita and Hynynen, 2005; Otani et al., 2009; Tsunoda et al., 2005). However, microbubbles have problems with size, stability, and targeting functionality.

Polyethyleneglycol (PEG)-modified liposomes have excellent biocompatibility, stability, and a long circulation time and can be easily prepared in a variety of sizes and modified to add a targeting function. For these reasons, they are widely used as carriers of drugs, antigens, and genes (Allen et al., 1991; Blume and Cevc, 1990; Harata et al., 2004; Maruyama et al., 1992, 2004). Therefore, PEG-liposomes containing a US imaging gas could be used as novel gene delivery agents. We recently reported that "Bubble liposomes" (BLs) were suitable for gene delivery *in vitro* and *in vivo* (Negishi et al., 2011b,c; Suzuki et al., 2007, 2008a,b). Furthermore, we showed that the combination of BLs and US was also useful for the delivery of siRNA *in vitro* and *in vivo* and that siRNA was introduced directly into the cytoplasm (Negishi et al., 2008). However, the results were obtained using a mixture of BLs and naked siRNA. With systemic injections, transfection efficiency is reduced if the BLs and siRNA are not colocalized in blood vessels. Therefore, it is important to control the biodistribution of both BLs and siRNA. In addition, siRNA is degraded by nuclease and removed rapidly from the circulation after intravenous administration. To overcome these problems, the loading of siRNA onto BLs could be effective for siRNA delivery. Recently, it has been reported that PEGylated lipoplexes (PEG-siPlex) bound to microbubbles led to an increase in the local lipoplex concentration near the cell membrane and resulted in much higher transfection with siRNA in the presence of US (Lentacker et al., 2009; Vandenbroucke et al., 2008). It was also shown that the delivery of siRNA by siRNA-microbubble complexes

* Corresponding author. Tel.: +81 42 676 3183; fax: +81 42 676 3183.
E-mail address: negishi@toyaku.ac.jp (Y. Negishi).
[1] These authors contributed equally to this work.

0378-5173/$ – see front matter © 2011 Elsevier B.V. All rights reserved.
doi:10.1016/j.ijpharm.2011.11.023

was effective for transfection into arteries (Suzuki et al., 2010). However, microbubbles were used in these reports. Microbubbles have problems with size, stability, and targeting functionality as mentioned above. Therefore, we developed nanosized, siRNA-loaded BLs using cholesterol-conjugated siRNA (chol-si-BLs) and demonstrated that using chol-si-BLs led to the stability of siRNA (Negishi et al., 2011a). In this study, we prepared siRNA-loaded BLs (si-BLs) using a cationic lipid. Novel si-BLs were able easily prepared compared with chol-si-BLs. Additionally, this method may have widespread utility for drug delivery systems because it is applicable to various materials possessing negative electrical charges. We also investigated the effects of the amount of PEG in the BLs on their interaction with siRNA, the stability of siRNA in serum, and the gene-silencing effects of transfection with si-BLs and US.

2. Materials and methods

2.1. Cell lines and cultures

COS-7 cells were cultured in Dulbecco's modified Eagle's medium (DMEM; Kohjin Bio Co. Ltd., Tokyo, Japan) supplemented with 10% heat-inactivated fetal bovine serum (FBS; Equitech Bio Inc., Kerrville, TX), 100 units/mL penicillin, and 100 μg/mL streptomycin in a humidified atmosphere containing 5% CO_2 at 37 °C.

2.2. Preparation of liposomes and BLs

To prepare liposomes for conventional BLs, 1,2-dipalmitoyl-sn-glycero-phosphatidylcholine (DPPC) and 1,2-distearoylphosphatidylethanolamine-methoxy-polyethylene glycol (PEG_{2000}) were mixed at a molar ratio of 94:6. Both lipids were purchased from NOF Corporation (Tokyo, Japan). 1,2-dioleoyl-3-trimethylammonium-propane (DOTAP) and 1,2-distearoyl-sn-glycero-3-phosphoethanolamine-N-[methoxy(polyethylene glycol)-750] (PEG_{750}) from Avanti Polar Lipids (Alabaster, AL) were also used. Liposomes with various lipid compositions were prepared by a reverse-phase evaporation method, as described previously (Negishi et al., 2008). In brief, all reagents were dissolved in 1:1 (v/v) chloroform/diisopropylether. Phosphate-buffered saline was added to the lipid solution, and the mixture was sonicated and then evaporated at 47 °C. The organic solvent was completely removed, and the size of the liposomes was adjusted to less than 200 nm using extruding equipment and a sizing filter (Nuclepore Track-Etch Membrane, 200 nm pore size, Whatman plc, UK). After being sized, the liposomes were passed through a sterile 0.45-μm syringe filter (Asahi Techno Glass Co., Chiba, Japan) to sterilize them. The lipid concentration was measured using the Phospholipid C test (Wako Pure Chemical Industries, Ltd., Osaka, Japan). BLs were prepared from liposomes and perfluoropropane gas (Takachiho Chemical Inc., Co., Ltd., Tokyo, Japan). First, 5-mL sterilized vials containing 2 mL of liposome suspension (lipid concentration: 1 mg/mL) were filled with perfluoropropane gas, capped, and then pressurized with 7.5 mL of perfluoropropane gas. The vials were placed in a bath-type sonicator (42 kHz, 100 W, Bransonic 2510J-DTH, Branson Ultrasonics Co., Danbury, CT) for 5 min to form BLs. The zeta potential and mean size of the BLs were determined using the light-scattering method with a zeta potential/particle sizer (Nicomp 380ZLS, Santa Barbara, CA).

2.3. Ultrasound imaging of BLs

BLs diluted with PBS were dispensed into 6-well plates. B-mode recordings were made using a high-frequency ultrasound imaging system (NP60R-UBM, Nepa Gene, Co., Ltd., Chiba, Japan).

2.4. Plasmid DNA and siRNA

The plasmid pCMV-GL3, derived from pGL3-basic (Promega, Madison, WI), is an expression vector encoding the firefly luciferase gene under the control of a cytomegalovirus promoter. Small interfering RNA targeting luciferase (Luciferase GL3 siRNA; siGL3) and a nontargeting siRNA (Control (non-sil.) siRNA; siCont) were purchased from Qiagen K.K. (Tokyo, Japan). Their sequences were as follows: siGL3, *5′-CUUACGCUGAGUACUUCGAdTdT-3′* and *5′-UCGAAGUACUCAGCGUAAGdTdT-3′*; siCont, *5′-UUCUCCGAACGUGUCACGUdTdT-3′* and *5′-ACGUGACACGUUCGGAGAAdTdT-3′*. Nontargeting fluorescein-labeled siRNA (BLOCK-iT Fluorescent Oligo) was purchased from Invitrogen Japan K.K. (Tokyo, Japan).

2.5. Preparation of si-BLs

For the preparation of si-BLs, adequate amounts of siRNA were added to BLs and gently mixed. FITC-labeled siRNA and flow cytometry were used to examine the interaction between siRNA and BLs. The fluorescence intensity of si-BLs was analyzed using a FACSCanto (Becton Dickinson, San Jose, CA). To quantify the amount of siRNA loaded onto the BL surfaces, the BLs were centrifuged at 2000 rpm for 1 min and the unbound siRNA was removed. The BL solution and the aqueous solution containing the unbound siRNA were then boiled for 5 min after which the optical density was measured at 260 nm using a spectrophotometer.

2.6. Stability of siRNA in serum

The BLs, siRNA, and si-BLs were incubated in 50% serum for 15, 30, and 60 min. Serum was used without heat inactivation. The stability of the siRNA was confirmed by 15% polyacrylamide gel electrophoresis. The gel was stained with SYBR SAFE (Invitrogen Japan K.K., Tokyo, Japan) and visualized under ultraviolet light.

2.7. Transfection of siRNA into cells using BLs or si-BLs

The mixture of siRNA (final concentration 100 nM) and BLs or si-BLs (60 μg) in culture medium containing 10% FBS was added to the cells transfected with pDNA on the previous day. The cells were immediately exposed to US (frequency, 2 MHz; duty, 50%; burst rate, 2.0 Hz; intensity 2.0 W/cm^2) for 10 s through a 6-mm diameter probe placed in the well. A Sonopore 3000 (NEPA GENE, Co., Ltd., Chiba, Japan) was used to generate the US. The cells were washed twice with culture medium and cultured for two days.

To measure luciferase activity after transfection, cell lysate was prepared with a lysis buffer (0.1 M Tris–HCl (pH 7.8), 0.1% Triton X-100, and 2 mM EDTA). Luciferase activity was measured using a luciferase assay system (Promega, Madison, WI) and a luminometer (LB96 V, Belthold Japan Co., Ltd., Tokyo, Japan). The activity is reported in as relative light units (RLU) per mg of protein.

2.8. Statistical analyses

All data are reported as the mean ± SD ($n = 4$). Data were considered significant when $P < 0.05$. The t-test was used to calculate statistical significance.

3. Results

3.1. Preparation of BLs containing DOTAP

Initial experiments were performed to investigate whether liposomes containing a cationic lipid, DOTAP, could entrap a US imaging gas as well as conventional BLs. We prepared liposomes containing DOTAP in various amounts and attempted to entrap the gas. The

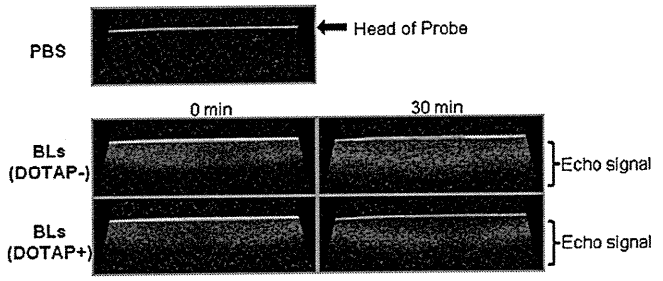

Fig. 1. Ultrasonographic images of a plate containing BLs with or without DOTAP.

liposomes containing up to 15 mol% DOTAP became cloudy, and we concluded that they could effectively entrap the imaging gas (data not shown). The liposomes containing more than 15 mol% DOTAP had difficulty entrapping the gas. We also examined BLs containing DOTAP using a high-frequency US imaging system. The system is a two-dimensional US image display composed of bright dots representing the US echoes. The brightness of each dot is determined by the amplitude of the returned echo signal. As shown in Fig. 1, the US echo signal was detected even 30 min later.

3.2. Effects of polyethyleneglycol on the interaction of siRNA with BLs

To assess whether siRNA could be loaded onto the surface of BLs, we used a fluorescence-activated cell sorter, the FACSCanto. We also prepared BLs containing different lengths of PEG to assess the effect of PEG on BL interactions with siRNA. As shown in Fig. 2, BLs not containing DOTAP were successfully loaded with siRNA. Approximately 40% of the BLs were FITC positive. Approximately 45% of the BLs containing DOTAP but not containing PEG_{750} were FITC positive. In contrast, BLs containing DOTAP and PEG_{750} were more heavily loaded with siRNA. Approximately 80% were FITC positive. Thus, in all subsequent experiments, BLs composed of DPPC, DOTAP, PEG_{2000}, and PEG_{750} (in a 79:15:3:3 molar ratio) were used.

Table 1
Size (nm) and zeta potential (mV) of BLs and si-BLs.

Lipid composition of BLs (molar ratio)	BLs	si-BLs
DPPC:PEG_{2000} = 94:6	528.3 nm	587.9 nm
DPPC:DOTAP:PEG_{2000}:PEG_{750} = 79:15:3:3	749.0 nm	862.2 nm
DPPC:PEG_{2000} = 94:6	−0.81 mV	−0.42 mV
DPPC:DOTAP:PEG_{2000}:PEG_{750} = 79:15:3:3	−0.20 mV	−0.13 mV

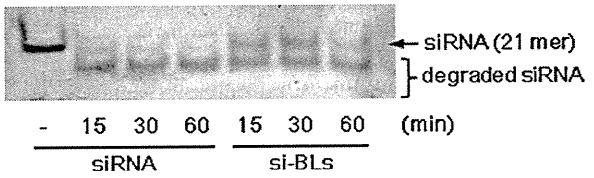

Fig. 3. Stability of siRNA in the presence of serum. Naked siRNA or si-BLs (DOTAP (+), PEG_{2000} and PEG_{750} (3:3)) were subjected to 50% serum degradation at 37 °C for 0.5 or 1 h and confirmed by 15% acrylamide gel electrophoresis.

As shown in Table 1, there was almost no change in the size and zeta potential of the BLs after siRNA was added.

We investigated the stability of siRNA in serum. Small interfering RNA held by BLs showed increased stability in 50% serum compared with free siRNA, although some siRNA was degraded (Fig. 3). We also examined the change in the amount of siRNA bound to BLs when the concentration of the siRNA was increased. As shown in Fig. 4, the amount siRNA loaded increased in a dose-dependent manner. We finally estimated that 60 μg of BLs could be loaded with at least 100 pmol of siRNA and that approximately 30% of the siRNA was bound to the lipid surface.

3.3. Transfection of siRNA into cells using BLs or si-BLs

Before the transfection experiments, we investigated the destruction efficiency of si-BLs under the US exposure. The solution of si-BLs was exposed to the same conditions used for *in vitro* transfection and was analyzed using the FACSCanto. Unlike the solution of si-BLs before US exposure, no fluorescence was detected in the

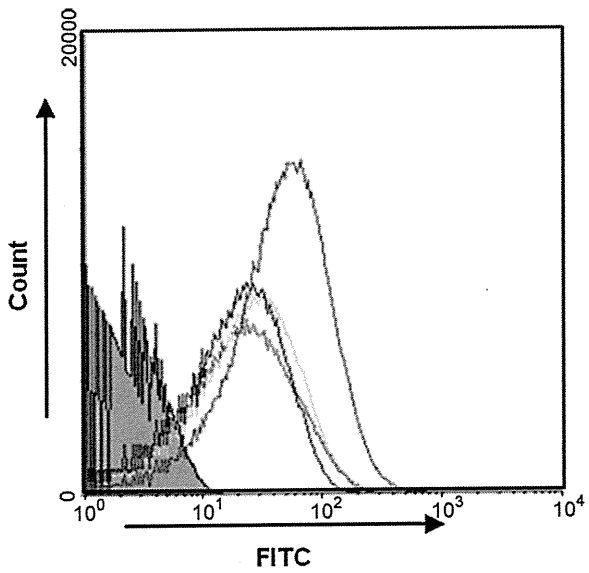

Fig. 2. Interaction of siRNA with BLs and the effects of PEG chain length on the interaction. The interaction was examined by analyzing a mixture of FITC-siRNA (50 pmol) and various BLs (60 μg) with the FACSCanto; gray area: BLs only; red curve: si-BLs (DOTAP (−), PEG_{2000} and PEG_{750} (molar ratio, 6:0)); green curve: si-BLs (DOTAP (+), PEG_{2000} and PEG_{750} (6:0)); blue curve: si-BLs (DOTAP (−), PEG_{2000} and PEG_{750} (3:3)); purple curve: si-BLs (DOTAP (+), PEG_{2000} and PEG_{750} (3:3)).

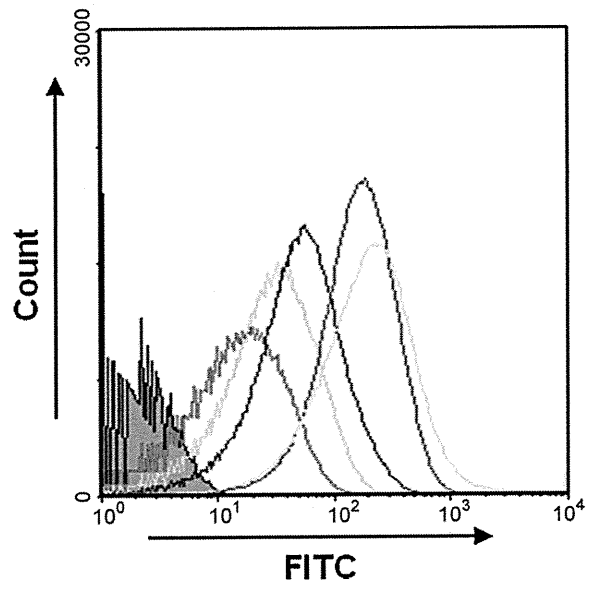

Fig. 4. Loading of siRNA onto BLs. The interaction was examined by analyzing a mixture of FITC-siRNA (12.5–200 pmol) and BLs (60 μg) containing DPPC, DOTAP, PEG_{2000} and PEG_{750} (79:15:3:3) with FACSCanto; gray area: BLs only; red curve: si-BLs (siRNA 12.5 pmol); green curve: si-BLs (siRNA 25 pmol); blue curve: si-BLs (siRNA 50 pmol); purple curve: s si-BLs (siRNA 100 pmol); light blue curve: si-BLs (siRNA 200 pmol).

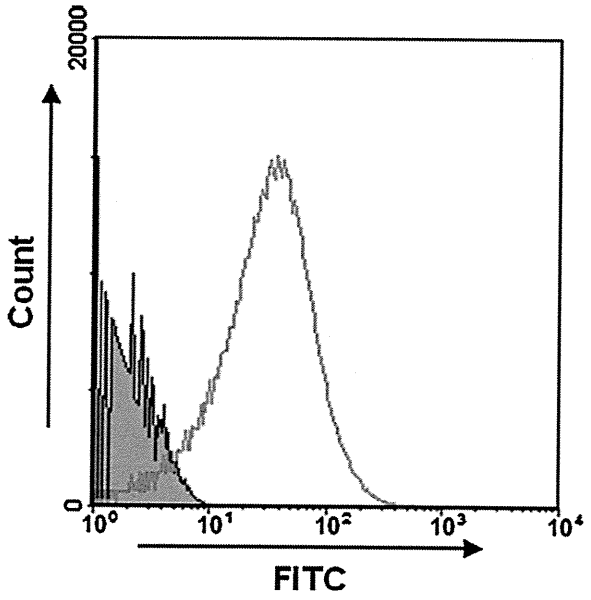

Fig. 5. Effects of US on si-BLs. The interaction was examined by analyzing a mixture of FITC-siRNA (50 pmol) and BLs (60 μg) containing DPPC, DOTAP, PEG_{2000}, and PEG_{750} (79:15:3:3) with the FACSCanto; gray area: BLs only; red curve: si-BLs; green curve: solution of si-BLs after US exposure (frequency, 2 MHz; duty, 50%; burst rate, 2.0 Hz; intensity, 2.0 W/cm^2; time, 10 s). (For interpretation of the references to color in this figure legend, the reader is referred to the web version of the article.)

solution (Fig. 5). This result suggested that the US caused the release of siRNA from the surface of the BLs.

To investigate the gene-silencing effects of siRNA transfection with si-BLs and US, cells transfected with pDNA encoding firefly luciferase (pCMV-GL3) on the previous day were added to BLs loaded with nontargeting control or luciferase-targeting siRNA (siCont or siGL3) and exposed to US (Fig. 6). Approximately 80% of luciferase expression was specifically blocked by siGL3 in the si-BLs-treated group and in the group treated with conventional BLs. Cytotoxicity was absent after the transfection with si-BLs and US (data not shown).

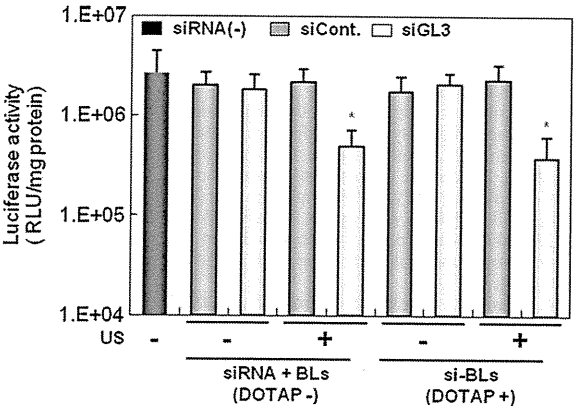

Fig. 6. Down-regulation of luciferase expression by siRNA with BL and US. COS-7 cells transfected with pCMV-GL3 on the previous day were added to siRNA (100 nM) and conventional BLs (DOTAP (−), PEG_{2000}, and PEG_{750} (molar ratio, 6:0)) or si-BLs (DOTAP (+), PEG_{2000}, and PEG_{750} (molar ratio, 3:3)) and applied. At 2 days posttransfection, luciferase expression was measured. siRNA(−); the group not transfected with siRNA, siCont; the group transfected with nontargeting siRNA (siCont), siGL3; the group transfected with siRNA targeting luciferase (siGL3). *P values <0.05 compared with the group transfected with siCont. All data are reported as the mean ± SD (n = 4).

4. Discussion

RNAi therapeutics have great potential for treating intractable diseases ranging from acquired diseases, such as viral infections, to purely genetic disorders. However, inefficient delivery into specific organs has hindered their clinical application.

Recently, a combination of microbubbles and US has been proposed as a less invasive and tissue-specific method of gene delivery. The combination produces transient changes in the permeability of the cell membrane and allows for the site-specific intracellular delivery of molecules such as dextran, pDNA, peptides, and siRNA both *in vitro* and *in vivo* (Du et al., 2011; Kinoshita and Hynynen, 2005; Li et al., 2003; Otani et al., 2009; Sonoda et al., 2006; Taniyama et al., 2002a,b; Tsunoda et al., 2005; Unger et al., 2004). However, because existing microbubbles have problems with size, stability, and targeting functionality, we developed liposomal bubbles (BLs). BLs are an effective and novel tool for gene and siRNA delivery *in vitro* and *in vivo* (Negishi et al., 2008, 2011b,c; Suzuki et al., 2007, 2008a,b). Our method using BLs and US did not involve endocytosis, and siRNA was directly introduced into the cytoplasm within a fairly short time. Thus, it seems unnecessary to consider the escape of siRNA from the endosome and the degradation of siRNA in lysosomes, although the endosomal escape is an important issue in other delivery tools. Furthermore transfection methods using physical energy other than US are expected and are currently being developed (Endoh and Ohtsuki, 2009; Kong et al., 2004; Oliveira et al., 2007; Schiffelers et al., 2005; Takei et al., 2008). These methods are difficult to apply to deep tissue. In contrast, US is able to control the accessible tissue sites by changing of the frequency and to reach the deep tissues. However, our previous results were obtained using a mixture of BLs and naked siRNA, which do not colocalize in blood vessels after intravenous administration. Additionally, siRNA is susceptible to degradation by nucleases and rapid removal from circulation. Consequently, these factors may cause a reduction in transfection efficiency. In this study, we prepared siRNA-loaded BLs (si-BLs) using a cationic lipid as a more effective, efficient delivery tool for systemic injections.

We initially attempted to entrap a US imaging gas in BLs containing DOTAP, a cationic lipid often used for gene delivery. Liposomes containing up to 15 mol% DOTAP did entrap the gas and could be used as ultrasound contrast agents. However, liposomes containing more than 15 mol% DOTAP had difficulty maintaining the gas. We also tested BLs containing DOTAP using a high-frequency US imaging system. An echo signal was detected as well as for BLs without DOTAP, although the imaging effect was slightly reduced 30 min later (Fig. 1). These results were assumed to be due to differences in the response to US and the stability of each BL type.

We used flow cytometry to examine the interaction between siRNA and BLs. The BLs were detectable, although the fluorescence intensity was low. The fluorescein-labeled siRNA molecules were too small to be detected with flow cytometry. However, the siRNA-loaded BLs exhibited strong fluorescence. We determined that siRNA could interact with BLs, and the interaction was due to the cationic charge of DOTAP. The amount of siRNA bound to the BLs was slightly increased in the presence of DOTAP. Furthermore, BLs containing both DOTAP and PEG_{750} could be loaded with much more siRNA (Fig. 2). BLs containing neither DOTAP nor PEG_{750} also loaded successfully with a certain amount of siRNA. These results suggested that siRNA could be loaded not only by the electrostatic interaction, but also by the fixed aqueous layer formed with PEG. It has been reported that the modification of liposomes with short and long PEG chains increases the fixed aqueous layer thickness (Sadzuka et al., 2002). We considered that the structural changes in the PEG chain facilitated interaction between the cationic lipid and anionic siRNA. Moreover, there were no significant changes in size after adding siRNA (Table 1). The data suggested that siRNA

was bound to the surface of BLs and that BLs did not aggregate. We also investigated the stability of siRNA interacting with BLs in 50% serum. Although some siRNA was degraded, siRNA held by BLs showed increased stability in 50% serum compared with free siRNA (Fig. 3). In the solution of si-BLs, free siRNA was present with si-BLs. Therefore, the siRNA not held by BLs was degraded. We examined the change in the amount of bound siRNA by adding various amounts of siRNA to BLs. As shown in Fig. 4, the amount of siRNA loaded onto BLs (60 μg) increased with siRNA addition in a dose-dependent manner up to 100 pmol.

We also investigated the effects of US exposure on si-BLs by analyzing the si-BL solution after exposure under the same conditions used for the *in vitro* transfection. No fluorescence was detected. Moreover, there were only a few detectable molecules in the solution of si-BLs after US exposure, and the histogram representing the results was almost parallel to the horizontal axis, similar to the solution of free siRNA (Fig. 5). This result suggested that US exposure collapsed si-BLs, releasing siRNA from the surface of the BLs. We confirmed that there was no damage to siRNA from US exposure by electrophoresis (data not shown). Undetectable fluorescence does not necessarily mean that siRNA were released from BLs: it is also possible that siRNA interacted with lipids or BLs that reverted to liposomes by degassing. However, the gene-silencing effects of siRNA transfection via si-BLs and US were comparable to those of siRNA transfection with conventional BLs and US (Fig. 6). Therefore, it appears that the exposure to US-induced cavitation, the release of siRNA from BLs, and the delivery of siRNA into the cytoplasm. We are currently developing BLs composed of lipids other than DPPC or DOTAP in attempts to form more stable and effective BLs. In the future, we will also examine siRNA delivery and disease-associated gene-silencing effects.

The preparation method of si-BLs developed in this study was easier than that of chol-si-BLs reported previously (Negishi et al., 2011a). Furthermore, BLs containing cationic lipid are expected to have widespread application to delivery tools of various molecules possessing negative electric charges. We confirmed that not only siRNA but also pDNA can be loaded onto BLs (p-BLs). Additionally, microbubbles conjugated to an antibody and having a targeting function have been developed recently (Behm et al., 2008; Leong-Poi et al., 2005; Palmowski et al., 2008). Liposomes can be easily modified to add a targeting function. Thus, the development of targeting si-BLs or p-BLs using an antibody or peptide is expected to lead to beneficial clinical applications for various diseases.

5. Conclusion

In this study, we showed that si-BLs could deliver siRNA as well as conventional BLs, although there remains room for improvement. Additionally, BLs containing a cationic lipid interacted with siRNA and protected the siRNA against nuclease degradation. These results suggest that si-BLs combined with US exposure may be useful for delivering siRNA to a tissue or organ via systemic injection.

Acknowledgements

We are grateful to Dr. Katsuro Tachibana (Department of Anatomy, School of Medicine, Fukuoka University) for technical advice regarding the induction of cavitation with US, to Ms. Yuko Ishii and Ms. Arisa Nakamura (School of Pharmacy, Tokyo University of Pharmacy and Life Sciences) for excellent technical assistance, and to Mr. Yasuhiko Hayakawa and Mr. Kosho Suzuki (Nepa Gege Co., Ltd.) for technical advice regarding US exposure. This study was supported by a Grant for Industrial Technology Research (04A05010) from the New Energy and Industrial Technology Development Organization (NEDO) of Japan, a Grant-in-Aid for Exploratory Research (18650146) from the Japan Society for the Promotion of Science, a Grant-in-Aid for Scientific Research (B) (20300179) from the Japan Society for the Promotion of Science, and a Grant-in-Aid for Young Scientists (B) (21790164) from the Japan Society for the Promotion of Science.

References

Allen, T.M., Hansen, C., Martin, F., Redemann, C., Yau-Young, A., 1991. Liposomes containing synthetic lipid derivatives of poly(ethylene glycol) show prolonged circulation half-lives in vivo. Biochim. Biophys. Acta 1066, 29–36.

Behm, C.Z., Kaufmann, B.A., Carr, C., Lankford, M., Sanders, J.M., Rose, C.E., Kaul, S., Lindner, J.R., 2008. Molecular imaging of endothelial vascular cell adhesion molecule-1 expression and inflammatory cell recruitment during vasculogenesis and ischemia-mediated arteriogenesis. Circulation 117, 2902–2911.

Blume, G., Cevc, G., 1990. Liposomes for the sustained drug release in vivo. Biochim. Biophys. Acta 1029, 91–97.

Delius, M., Adams, G., 1999. Shock wave permeabilization with ribosome inactivating proteins: a new approach to tumor therapy. Cancer Res. 59, 5227–5232.

Du, J., Shi, Q.S., Sun, Y., Liu, P.F., Zhu, M.J., Du, L.F., Duan, Y.R., 2011. Enhanced delivery of monomethoxypoly(ethylene glycol)-poly(lactic-co-glycolic acid)-poly l-lysine nanoparticles loading platelet-derived growth factor BB small interfering RNA by ultrasound and/or microbubbles to rat retinal pigment epithelium cells. J. Gene Med. 13, 312–323.

Duvshani-Eshet, M., Machluf, M., 2005. Therapeutic ultrasound optimization for gene delivery: a key factor achieving nuclear DNA localization. J. Control. Release 108, 513–528.

Endoh, T., Ohtsuki, T., 2009. Cellular siRNA delivery using cell-penetrating peptides modified for endosomal escape. Adv. Drug Deliv. Rev. 61, 704–709.

Frank-Kamenetsky, M., Grefhorst, A., Anderson, N.N., Racie, T.S., Bramlage, B., Akinc, A., Butler, D., Charisse, K., Dorkin, R., Fan, Y., Gamba-Vitalo, C., Hadwiger, P., Jayaraman, M., John, M., Jayaprakash, K.N., Maier, M., Nechev, L., Rajeev, K.G., Read, T., Röhl, I., Soutschek, J., Tan, P., Wong, J., Wang, G., Zimmermann, T., de Fougerolles, A., Vornlocher, H.P., Langer, R., Anderson, D.G., Manoharan, M., Koteliansky, V., Horton, J.D., Fitzgerald, K., 2008. Therapeutic RNAi targeting PCSK9 acutely lowers plasma cholesterol in rodents and LDL cholesterol in nonhuman primates. Proc. Natl. Acad. Sci. U.S.A. 105, 11915–11920.

Greenleaf, W.J., Bolander, M.E., Sarkar, G., Goldring, M.B., Greenleaf, J.F., 1998. Artificial cavitation nuclei significantly enhance acoustically induced cell transfection. Ultrasound Med. Biol. 24, 587–595.

Halder, J., Kamat, A.A., Landen, C.N., Han, L.Y., Lutgendorf, S.K., Lin, Y.G., Merritt, W.M., Jennings, N.B., Chavez-Reyes, A., Coleman, R.L., Gershenson, D.M., Schmandt, R., Cole, S.W., Lopez-Berestein, G., Sood, A.K., 2006. Focal adhesion kinase targeting using *in vivo* short interfering RNA delivery in neutral liposomes for ovarian carcinoma therapy. Clin Cancer Res. 12, 4916–4924.

Harata, M., Soda, Y., Tani, K., Ooi, J., Takizawa, T., Chen, M., Bai, Y., Izawa, K., Kobayashi, S., Tomonari, A., Nagamura, F., Takahashi, S., Uchimaru, K., Iseki, T., Tsuji, T., Takahashi, T.A., Sugita, K., Nakazawa, S., Tojo, A., Maruyama, K., Asano, S., 2004. CD19-targeting liposomes containing imatinib efficiently kill Philadelphia chromosome-positive acute lymphoblastic leukemia cells. Blood 104, 1442–1449.

Holmes, R.P., Yeaman, L.D., Taylor, R.G., McCullough, D.L., 1992. Altered neutrophil permeability following shock wave exposure *in vitro*. J. Urol. 147, 733–737.

Kim, S.H., Jeong, J.H., Lee, S.H., Kim, S.W., Park, T.G., 2008. Local and systemic delivery of VEGF siRNA using polyelectrolyte complex micelles for effective treatment of cancer. J. Control. Release 129, 107–116.

Kinoshita, M., Hynynen, K., 2005. A novel method for the intracellular delivery of siRNA using microbubble-enhanced focused ultrasound. Biochem. Biophys. Res. Commun. 335, 393–399.

Kong, X.C., Barzaghi, P., Ruegg, M.A., 2004. Inhibition of synapse assembly in mammalian muscle *in vivo* by RNA interference. EMBO Rep. 5, 183–188.

Lentacker, I., Wang, N., Vandenbroucke, R.E., Demeester, J., De Smedt, S.C., Sanders, N.N., 2009. Ultrasound exposure of lipoplex loaded microbubbles facilitates direct cytoplasmic entry of the lipoplexes. Mol. Pharm. 6, 457–467.

Leong-Poi, H., Christiansen, J., Heppner, P., Lewis, C.W., Klibanov, A.L., Kaul, S., Lindner, J.R., 2005. Assessment of endogenous and therapeutic arteriogenesis by contrast ultrasound molecular imaging of integrin expression. Circulation 111, 3248–3254.

Li, T., Tachibana, K., Kuroki, M., Kuroki, M., 2003. Gene transfer with echo-enhanced contrast agents: comparison between Albunex, Optison, and Levovist in mice—initial results. Radiology 229, 423–428.

Maruyama, K., Ishida, O., Kasaoka, S., Takizawa, T., Utoguchi, N., Shinohara, A., Chiba, M., Kobayashi, H., Eriguchi, M., Yanagie, H., 2004. Intracellular targeting of sodium mercaptoundecahydrododecaborate (BSH) to solid tumors by transferrin-PEG liposomes, for boron neutron-capture therapy (BNCT). J. Control. Release 98, 195–207.

Maruyama, K., Yuda, T., Okamoto, A., Kojima, S., Suginaka, A., Iwatsuru, M., 1992. Prolonged circulation time in vivo of large unilamellar liposomes composed of distearoyl phosphatidylcholine and cholesterol containing amphipathic poly(ethylene glycol). Biochim. Biophys. Acta 1128, 44–49.

McCaffrey, A.P., Meuse, L., Pham, T.T., Conklin, D.S., Hannon, G.J., Kay, M.A., 2002. RNA interference in adult mice. Nature 418, 38–39.

Morrissey, D.V., Lockridge, J.A., Shaw, L., Blanchard, K., Jensen, K., Breen, W., Hartsough, K., Machemer, L., Radka, S., Jadhav, V., Vaish, N., Zinnen, S., Vargeese, C.,

Bowman, K., Shaffer, C.S., Jeffs, L.B., Judge, A., MacLachlan, I., Polisky, B., 2005. Potent and persistent *in vivo* anti-HBV activity of chemically modified siRNAs. Nat. Biotechnol. 23, 1002–1007.

Negishi, Y., Endo-Takahashi, Y., Ishii, K., Suzuki, R., Oguri, Y., Murakami, T., Maruyama, K., Aramaki, Y., 2011a. Development of novel nucleic acid-loaded Bubble liposomes using cholesterol-conjugated siRNA. J. Drug Target 19, 830–836.

Negishi, Y., Endo, Y., Fukuyama, T., Suzuki, R., Takizawa, T., Omata, D., Maruyama, K., Aramaki, Y., 2008. Delivery of siRNA into the cytoplasm by liposomal bubbles and ultrasound. J. Control. Release 132, 124–130.

Negishi, Y., Matsuo, K., Endo-Takahashi, Y., Suzuki, K., Matsuki, Y., Takagi, N., Suzuki, R., Maruyama, K., Aramaki, Y., 2011b. Delivery of an angiogenic gene into ischemic muscle by novel bubble liposomes followed by ultrasound exposure. Pharm. Res. 28, 712–719.

Negishi, Y., Tsunoda, Y., Endo-Takahashi, Y., Oda, Y., Suzuki, R., Maruyama, K., Yamamoto, M., Aramaki, Y., 2011c. Local gene delivery system by bubble liposomes and ultrasound exposure into joint synovium. J. Drug Deliv. 2011, 203986.

Niu, X.Y., Peng, Z.L., Duan, W.Q., Wang, H., Wang, P., 2006. Inhibition of HPV 16 E6 oncogene expression by RNA interference *in vitro* and *in vivo*. Int. J. Gynecol. Cancer 16, 743–751.

Oliveira, S., Fretz, M.M., Høgset, A., Storm, G., Schiffelers, R.M., 2007. Photochemical internalization enhances silencing of epidermal growth factor receptor through improved endosomal escape of siRNA. Biochim. Biophys. Acta 1768, 1211–1217.

Otani, K., Yamahara, K., Ohnishi, S., Obata, H., Kitamura, S., Nagaya, N., 2009. Nonviral delivery of siRNA into mesenchymal stem cells by a combination of ultrasound and microbubbles. J. Control. Release 133, 146–153.

Palmowski, M., Huppert, J., Ladewig, G., Hauff, P., Reinhardt, M., Mueller, M.M., Woenne, E.C., Jenne, J.W., Maurer, M., Kauffmann, G.W., Semmler, W., Kiessling, F., 2008. Molecular profiling of angiogenesis with targeted ultrasound imaging: early assessment of antiangiogenic therapy effects. Mol. Cancer Ther. 7, 101–109.

Sadzuka, Y., Nakade, A., Hirama, R., Miyagishima, A., Nozawa, Y., Hirota, S., Sonobe, T., 2002. Effects of mixed polyethyleneglycol modification on fixed aqueous layer thickness and antitumor activity of doxorubicin containing liposome. Int. J. Pharm. 238, 171–180.

Sato, Y., Murase, K., Kato, J., Kobune, M., Sato, T., Kawano, Y., Takimoto, R., Takada, K., Miyanishi, K., Matsunaga, T., Takayama, T., Niitsu, Y., 2008. Resolution of liver cirrhosis using vitamin A-coupled liposomes to deliver siRNA against a collagen-specific chaperone. Nat. Biotechnol. 26, 431–442.

Schiffelers, R.M., Xu, J., Storm, G., Woodle, M.C., Scaria, P.V., 2005. Effects of treatment with small interfering RNA on joint inflammation in mice with collagen-induced arthritis. Arthritis Rheum. 52, 1314–1318.

Schratzberger, P., Krainin, J.G., Schratzberger, G., Silver, M., Ma, H., Kearney, M., Zuk, R.F., Brisken, A.F., Losordo, D.W., Isner, J.M., 2002. Transcutaneous ultrasound augments naked DNA transfection of skeletal muscle. Mol. Ther. 6, 576–583.

Song, E., Lee, S.K., Wang, J., Ince, N., Ouyang, N., Min, J., Chen, J., Shankar, P., Lieberman, J., 2003. RNA interference targeting Fas protects mice from fulminant hepatitis. Nat. Med. 9, 347–351.

Sonoda, S., Tachibana, K., Uchino, E., Okubo, A., Yamamoto, M., Sakoda, K., Hisatomi, T., Sonoda, K.H., Negishi, Y., Izumi, Y., Takao, S., Sakamoto, T., 2006. Gene transfer to corneal epithelium and keratocytes mediated by ultrasound with microbubbles. Invest. Ophthalmol. Vis. Sci. 47, 558–564.

Suzuki, J., Ogawa, M., Takayama, K., Taniyama, Y., Morishita, R., Hirata, Y., Nagai, R., Isobe, M., 2010. Ultrasound-microbubble-mediated intercellular adhesion molecule-1 small interfering ribonucleic acid transfection attenuates neointimal formation after arterial injury in mice. J. Am. Coll. Cardiol. 55, 904–913.

Suzuki, R., Takizawa, T., Negishi, Y., Hagisawa, K., Tanaka, K., Sawamura, K., Utoguchi, N., Nishioka, T., Maruyama, K., 2007. Gene delivery by combination of novel liposomal bubbles with perfluoropropane and ultrasound. J. Control. Release 117, 130–136.

Suzuki, R., Takizawa, T., Negishi, Y., Utoguchi, N., Maruyama, K., 2008a. Effective gene delivery with novel liposomal bubbles and ultrasonic destruction technology. Int. J. Pharm. 354, 49–55.

Suzuki, R., Takizawa, T., Negishi, Y., Utoguchi, N., Sawamura, K., Tanaka, K., Namai, E., Oda, Y., Matsumura, Y., Maruyama, K., 2008b. Tumor specific ultrasound enhanced gene transfer *in vivo* with novel liposomal bubbles. J. Control. Release 125, 137–144.

Takei, Y., Nemoto, T., Mu, P., Fujishima, T., Ishimoto, T., Hayakawa, Y., Yuzawa, Y., Matsuo, S., Muramatsu, T., Kadomatsu, K., 2008. *In vivo* silencing of a molecular target by short interfering RNA electroporation: tumor vascularization correlates to delivery efficiency. Mol. Cancer Ther. 7, 211–221.

Takeshita, F., Minakuchi, Y., Nagahara, S., Honma, K., Sasaki, H., Hirai, K., Teratani, T., Namatame, N., Yamamoto, Y., Hanai, K., Kato, T., Sano, A., Ochiya, T., 2005. Efficient delivery of small interfering RNA to bone-metastatic tumors by using atelocollagen *in vivo*. Proc. Natl. Acad. Sci. U.S.A. 102, 12177–12182.

Taniyama, Y., Tachibana, K., Hiraoka, K., Aoki, M., Yamamoto, S., Matsumoto, K., Nakamura, T., Ogihara, T., Kaneda, Y., Morishita, R., 2002a. Development of safe and efficient novel nonviral gene transfer using ultrasound: enhancement of transfection efficiency of naked plasmid DNA in skeletal muscle. Gene Ther. 9, 372–380.

Taniyama, Y., Tachibana, K., Hiraoka, K., Namba, T., Yamasaki, K., Hashiya, N., Aoki, M., Ogihara, T., Yasufumi, K., Morishita, R., 2002b. Local delivery of plasmid DNA into rat carotid artery using ultrasound. Circulation 105, 1233–1239.

Tsunoda, S., Mazda, O., Oda, Y., Iida, Y., Akabame, S., Kishida, T., Shin-Ya, M., Asada, H., Gojo, S., Imanishi, J., Matsubara, H., Yoshikawa, T., 2005. Sonoporation using microbubble BR14 promotes pDNA/siRNA transduction to murine heart. Biochem. Biophys. Res. Commun. 336, 118–127.

Unger, E.C., Porter, T., Culp, W., Labell, R., Matsunaga, T., Zutshi, R., 2004. Therapeutic applications of lipid-coated microbubbles. Adv. Drug Deliv. Rev. 56, 1291–1314.

Vandenbroucke, R.E., Lentacker, I., Demeester, J., De Smedt, S.C., Sanders, N.N., 2008. Ultrasound assisted siRNA delivery using PEG-siPlex loaded microbubbles. J. Control. Release 126, 265–273.

Xia, C.F., Zhang, Y., Zhang, Y., Boado, R.J., Pardridge, W.M., 2007. Intravenous siRNA of brain cancer with receptor targeting and avidin-biotin technology. Pharm. Res. 24, 2309–2316.